Supporting Information

An Activated Coumarin Michael Acceptor for CN^-

Aaron B. Davis[(a)], Rachel E. Lambert[(a)], Frank R. Fronczek[(b)], Peter J. Cragg[(c)] and Karl J. Wallace*[(a)]

(a) Department of Chemistry and Biochemistry University of Southern Mississippi, Hattiesburg, Mississippi 39406, United States (b) Department of Chemistry, Louisiana State University, , Baton Rouge, Louisiana, 70803, United States (c) School of Pharmacy and Biomolecular Sciences, University of Brighton, Brighton BN2 4GJ United Kingdom

Tautomers and numbering scheme…….…….. Page 2

Solvent polarity factor…..... Page 2-4

UV-vis studies…….…. Page 5-9

Fluorescence studies……. Page 9-14

ESI mass spectrometry……... Page 14

NMR studies of compound **3**…… Page 15-27

NMR studies of **3-CN** adduct……..… Page 28-37

Jobs plot…….. Page 38

Detection limit (LOD)……. Page 38

Kinetic studies…… Page 39

Molecular modelling……. Page 40-42

X-Ray crystallography…….. Page 42-47

References…… Page 48

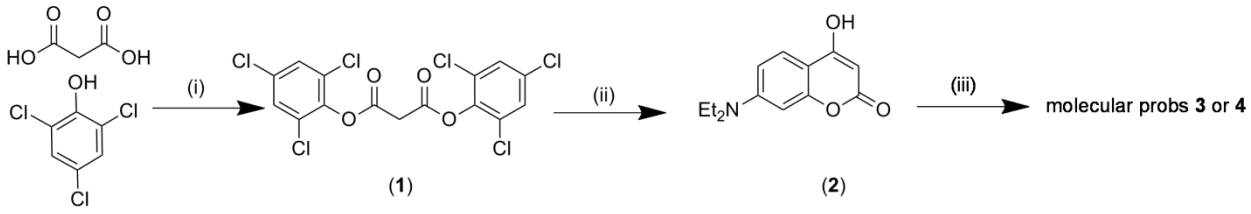

Scheme S1: The synthesis of the coumarin common intermediate (**2**): (i) phosphorus(v)oxychloride; (ii) 3-diethylaminophenol in toluene and (iii) one equivalent of amine, 1.5 equivalents of triethylortho formate and propan-2-ol.

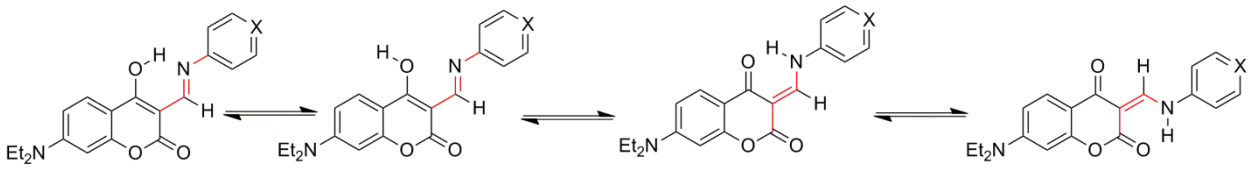

Scheme S2: Potential isomers and tautomers for compounds **3** and **4**. The existence of two species in solution in approximate 70:30 ratio in DMSO-d_6 is observed for *E*-(keto) enamine *Z*-(keto) enamine.

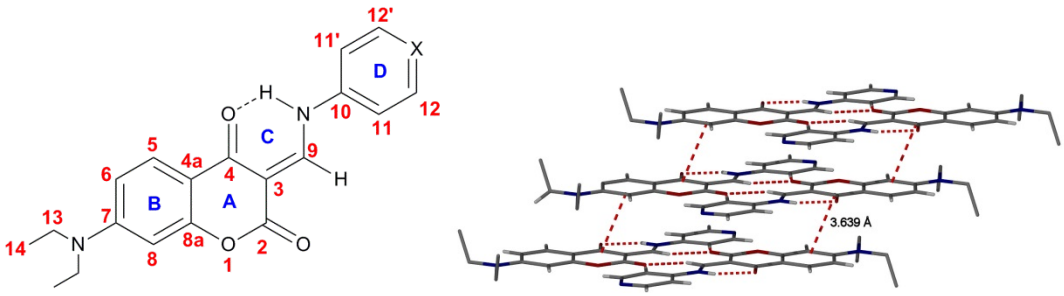

Figure S1: (Left) Numbering system and ring labeling system used in this work (right) X-ray packing highlighting the π-π stacking (3.639 Å).

Solvent polarity factor: The organic solvents used for the calculation of the polarity factor (ΔF) were of spectroscopic grade. Dielectric constant (ε) and refractive index (n) were taken from literature.[1] Following Lippert and Mataga the polarity factor was estimated using the following equation.

$$\Delta F = \frac{\varepsilon - 1}{2\varepsilon + 1} - \frac{n^2 - 1}{2n^2 + 1} \qquad \text{(equation } \mathbf{1}\text{)}$$

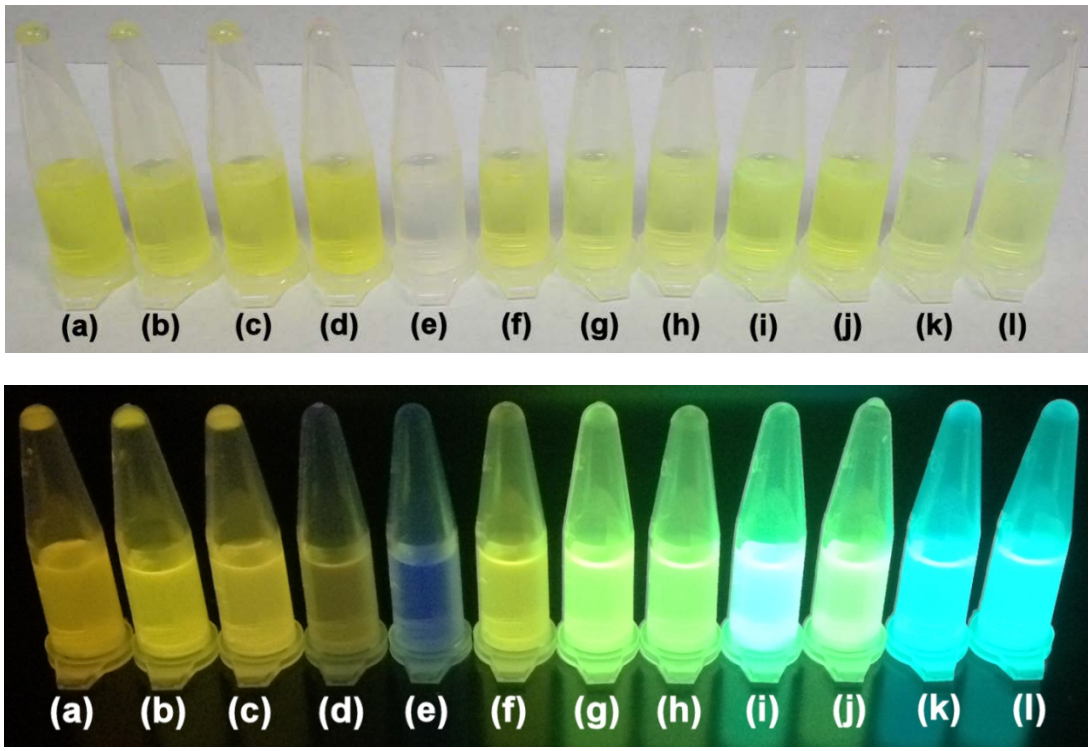

Figure S2: Compound **3** (3.0×10^{-4} $moldm^{-3}$) (a) DMSO, (b) MeCN, (c) DMF, (d) MeOH, (e) EtOH, (f) acetone, (g) THF, (h) EtOAc, (i) $CHCl_3$, (j) CH_2Cl_2, (k) toluene, (l) benzene.

Table S1: Absorption and fluorescence emission of molecular probe **3** in various solvents ($\lambda_{ex} = \lambda_{abs}$; room temperature; *16 $\mu moldm^{-3}$*).

	Solvent	Dielectric constant	λ_{max}^{abs} (nm)	λ_{max}^{em} (nm)	Stokes Shift	ΔF
(a)	dimethyl sulfoxide*	46.7	401	574	173	0.263
(b)	acetonitrile*	37.5	401	561	160	0.305
(c)	*N, N*-dimethyl formamide*	36.7	402	577	175	0.274
(d)	methanol$^{\$}$	32.7	406	573	167	0.309
(e)	ethanol$^{\$}$	24.5	343	385	42	0.289
(f)	acetone*	20.7	401	549	148	0.284
(g)	tetrahydrofuran*	7.6	401	520	119	0.210
(h)	ethyl acetate*	6.0	400	520	120	0.199
(i)	chloroform^{+}	4.8	415	491	76	0.148
(j)	dichloromethane^{+}	8.9	411	510	99	0.217
(k)	toluene^{+}	2.4	406	473	67	0.015
(l)	benzene^{+}	2.3	406	484	78	0.005

***** polar aprotic; $^{\$}$ polar protic; $^{+}$ non-polar

Table S2: Absorption and fluorescence emission of molecular probe **4** in various solvents ($\lambda_{ex} = \lambda_{abs}$; room temperature; *16 μmoldm^{-3}*).

	Solvent	Dielectric constant	$\lambda\frac{abs}{max}$ (nm)	$\lambda\frac{em}{max}$ (nm)	Stokes Shift	ΔF
(a)	dimethyl sulfoxide*	46.7	398	542	144	0.263
(b)	acetonitrile*	37.5	394	519	125	0.305
(c)	*N, N*-dimethyl formamide*	36.7	396	526	130	0.274
(d)	methanol$^{\$}$	32.7	397	511	114	0.309
(e)	ethanol$^{\$}$	24.5	399	516	117	0.289
(f)	acetone*	20.7	394	511	117	0.284
(g)	tetrahydrofuran*	7.6	394	484	90	0.210
(h)	ethyl acetate*	6.0	392	480	88	0.199
(i)	chloroform^{+}	4.8	399	460	61	0.148
(j)	dichloromethane^{+}	8.9	398	480	82	0.217
(k)	toluene^{+}	2.4	395	449	54	0.015
(l)	benzene^{+}	2.3	396	457	61	0.005

(A) (B)

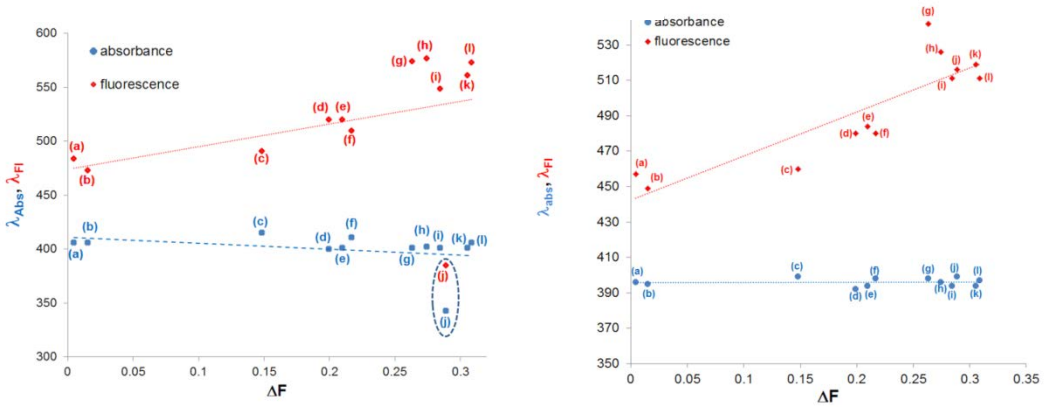

*Figure S3: (A) Absorption and emission maxima of probe **3** and (B) Absorption and emission maxima of probe **4** in various solvents (16 μmoldm^{-3}, 25 ℃). a) benzene b) toluene c) chloroform d) ethyl acetate e) THF f) dichloromethane g) DMSO h) DMF i) acetone J) ethanol k) acetonitrile and l) methanol. As a note, the behavior of ethanol is a strange phenomenon; a number of coumarin-enamine derivatives have been prepared and we are currently investigating their solvatochromic effect. It is possible that the water content in the ethanol is affecting the behavior.*

UV-Vis studies (General procedure): A stock solution of molecular probes **3** or **4** (3.1 mmoldm^{-3}) was prepared by dissolving 21 mg in 20 mL DMSO. From this stock solution a 16 μM solution of probes **3** or **4** was prepared in a one mL quartz cell for the UV-Vis spectroscopic studies. Anion stock solutions (3.1 mM) were also prepared in DMSO. These where then diluted in a 10 mL DMSO solution (311 μM). Aliquots of 5 μL of the anion was added to the UV-Vis cell (each 5 μL addition ≡ 0.1 equivalents of anion).

Table S4. UV-Vis data for compounds **3** and **4**.

Compound	**$CHCl_3$** λ_{max} **(ε)***	**EtOH** λ_{max} **(ε)***	**DMSO** λ_{max} **(ε)***	**DMSO:H_2O** λ_{max} **(ε)***
3	415 (38,723)	342 (43,654)	404 (44,387)	348 (25,599)
4	402 (50,460)	400 (62,485)	398 (51,963)	398 (57,150)

λ_{max} in nm; (ε) in Lmol^{-1}cm^{-1}

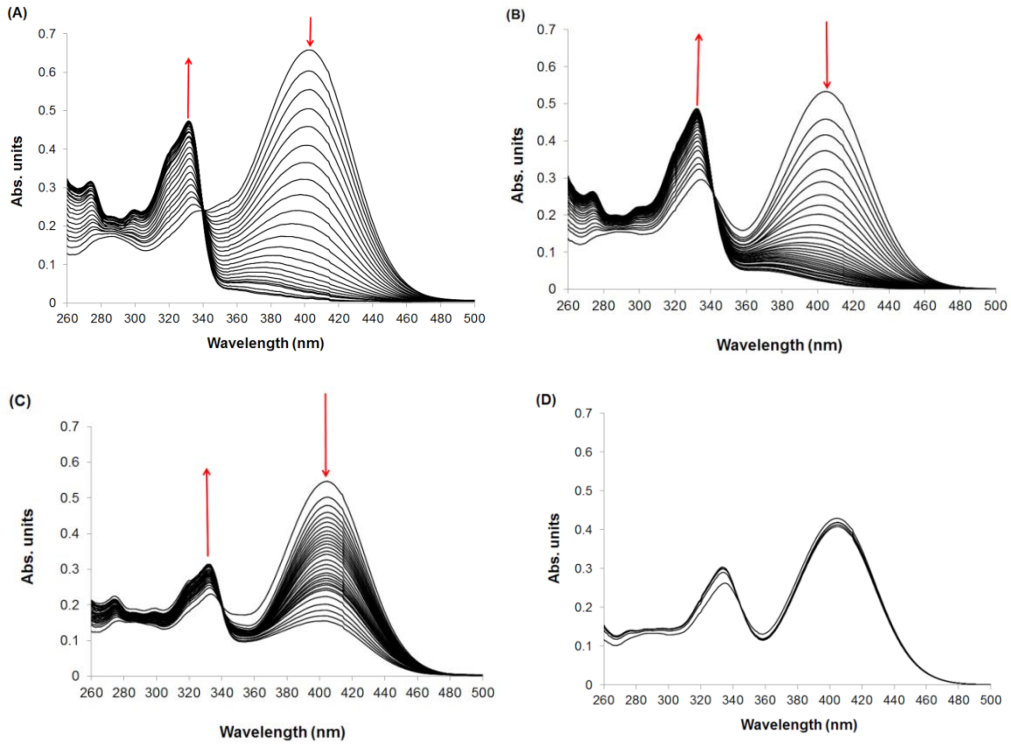

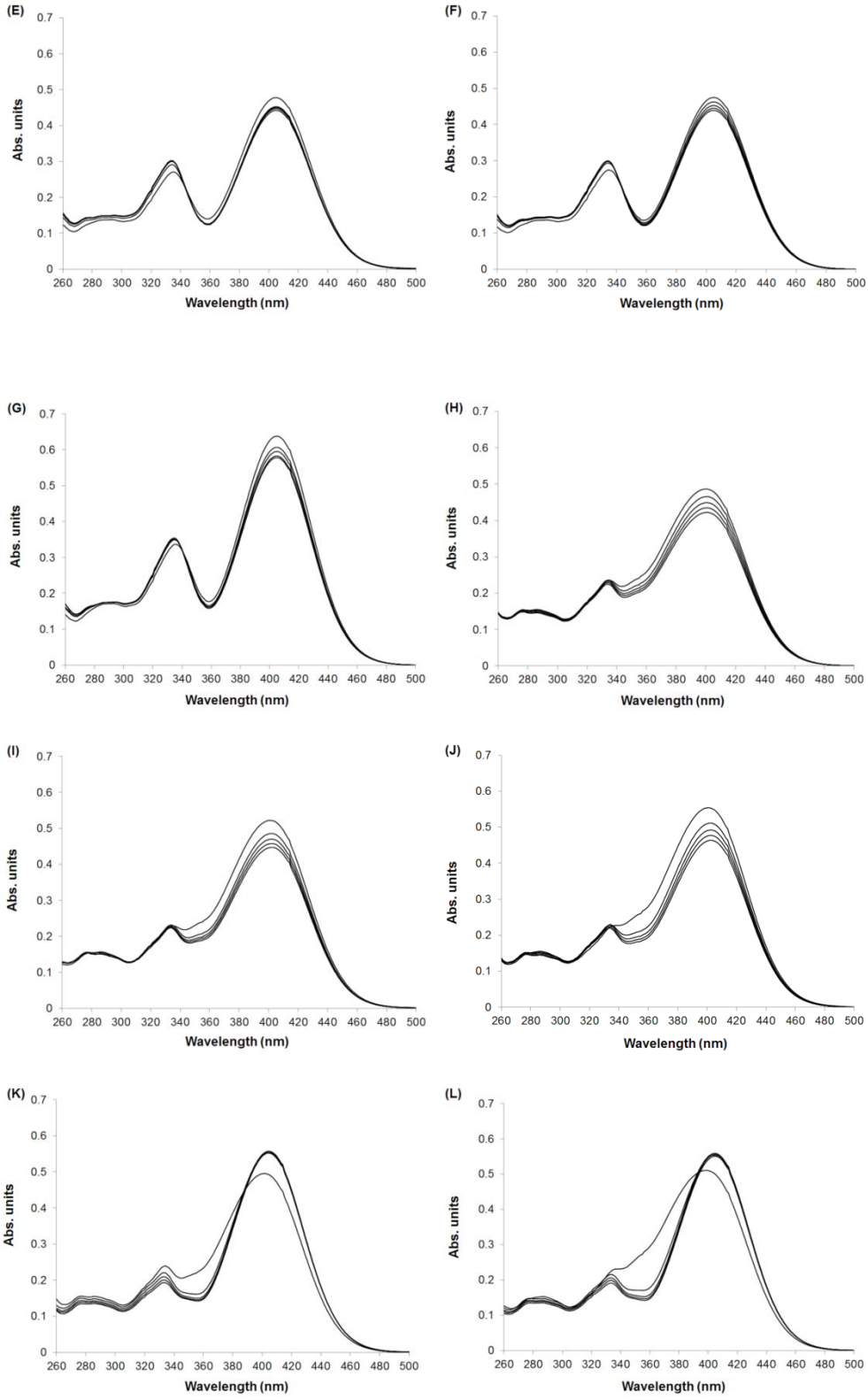
(E)
(F)
(G)
(H)
(I)
(J)
(K)
(L)
Abs. units
Wavelength (nm)
0
0.1
0.2
0.3
0.4
0.5
0.6
0.7
260 280 300 320 340 360 380 400 420 440 460 480 500

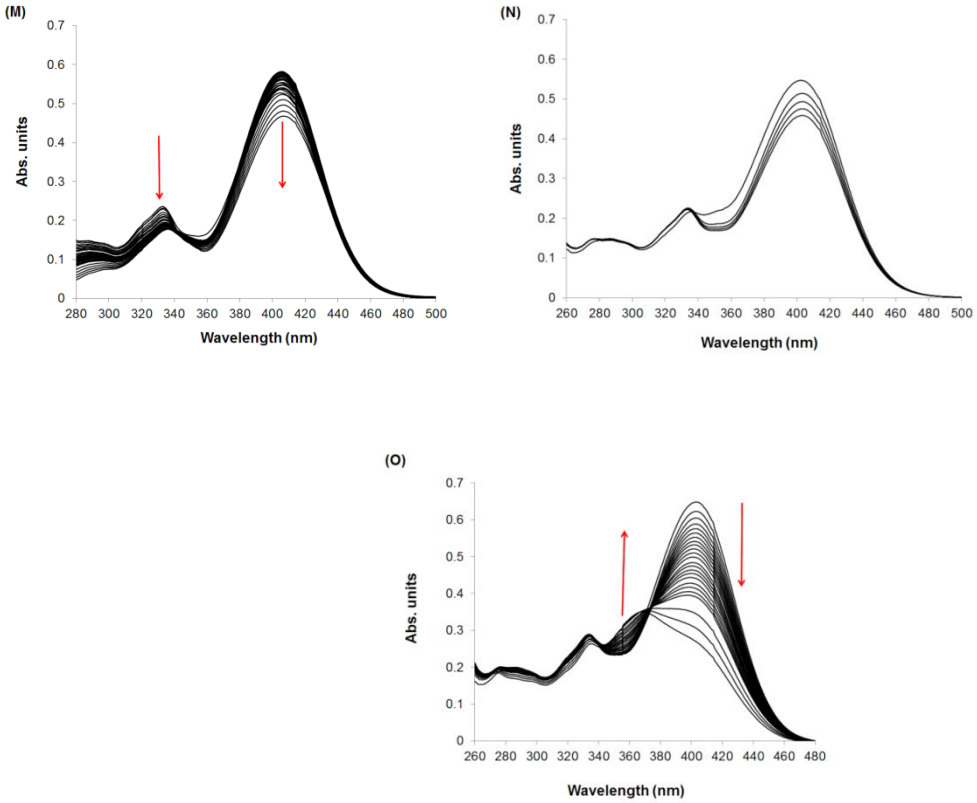

Figure S4: UV-Vis response of molecular probe **3** upon the addition of the following anions (15.6 mmoldm^{-3} in DMSO): (A) KCN (B) TBAF (C) $TBAH_2PO_4$ (D) TBABr (E) TBACl (F) TBAI (G) $TBANO_3$ (H) $NaBF_4$ (I) NaN_3 (J) $TBAHSO_4$ (K) NH_4SCN (L) NH_4ClO_4 (M) $TBACH_3CO_2$ (N) NH_4OH and (O) octylamine.

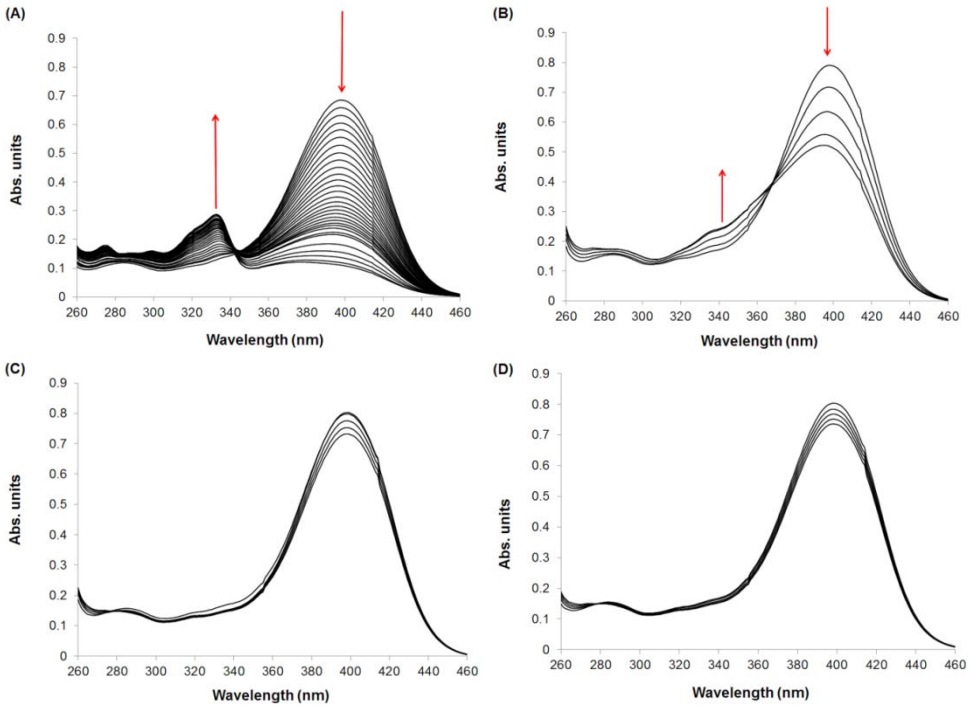

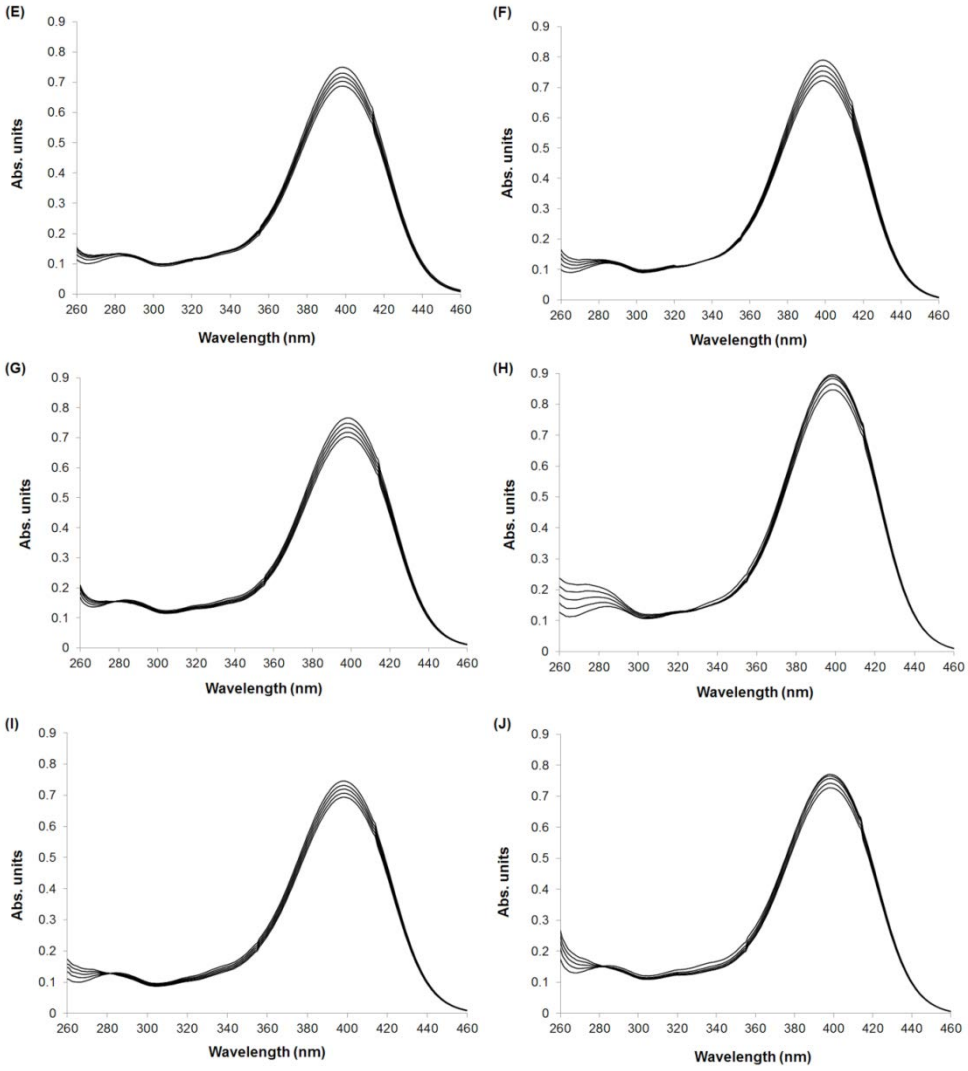
(E)
(F)
(G)
(H)
(I)
(J)
Abs. units
Wavelength (nm)
0
0.1
0.2
0.3
0.4
0.5
0.6
0.7
0.8
0.9
260
280
300
320
340
360
380
400
420
440
460

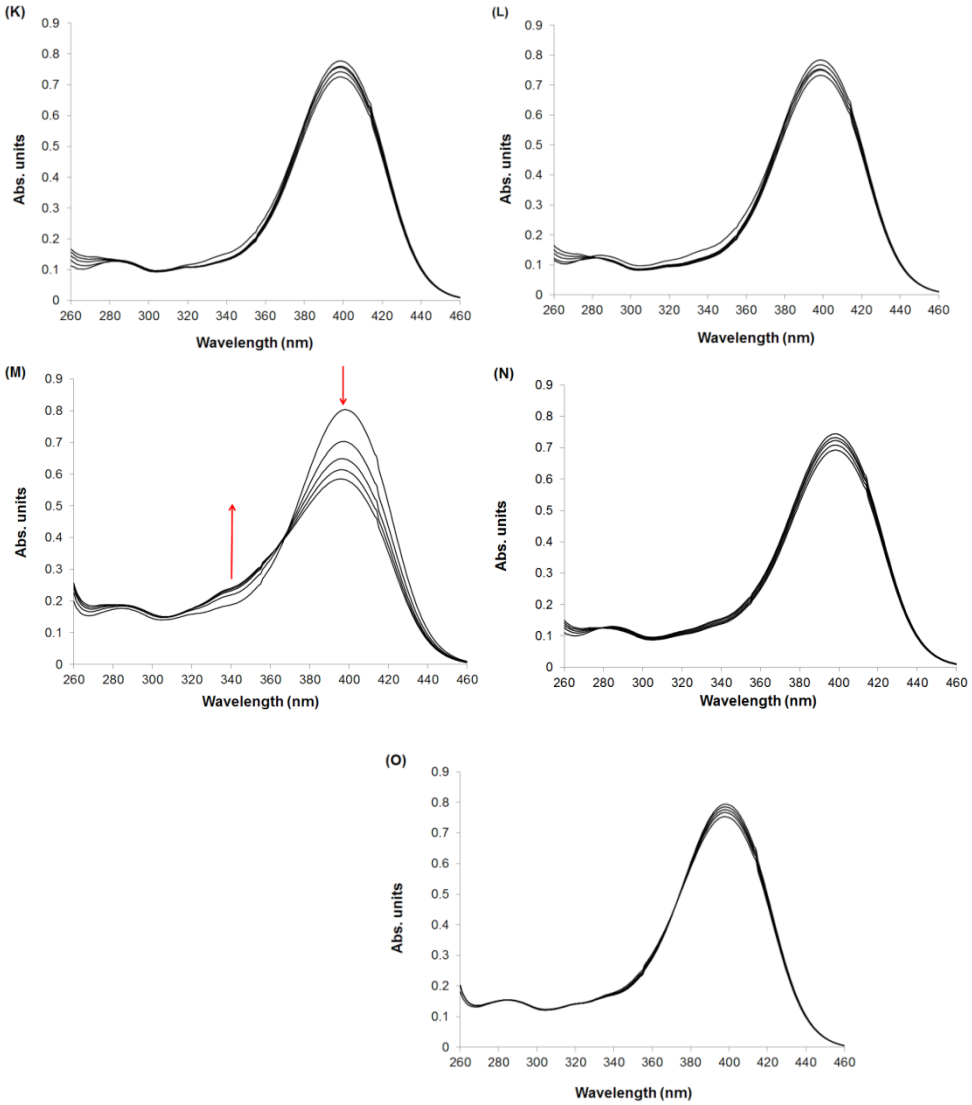

Figure S5: UV-Vis response of molecular probe **4** upon the addition of the following anions (15.6 mmoldm^{-3} in DMSO): (A) KCN (B) TBAF (C) $TBAH_2PO_4$ (D) TBABr (E) TBACl (F) TBAI (G) $TBANO_3$ (H) $NaBF_4$ (I) NaN_3 (J) $TBAHSO_4$ (K) NH_4SCN (L) NH_4ClO_4 (M) $TBACH_3CO_2$ (N) NH_4OH and (O) octylamine.

Fluorescence Studies: For all fluorescence studies stock solution were prepared. Compounds **3** and **4** were then diluted by removing 100 μL and diluting to 2 mL. Aliquots of 10 μL of the anion was added, equivalent to 0.1 equivalences.

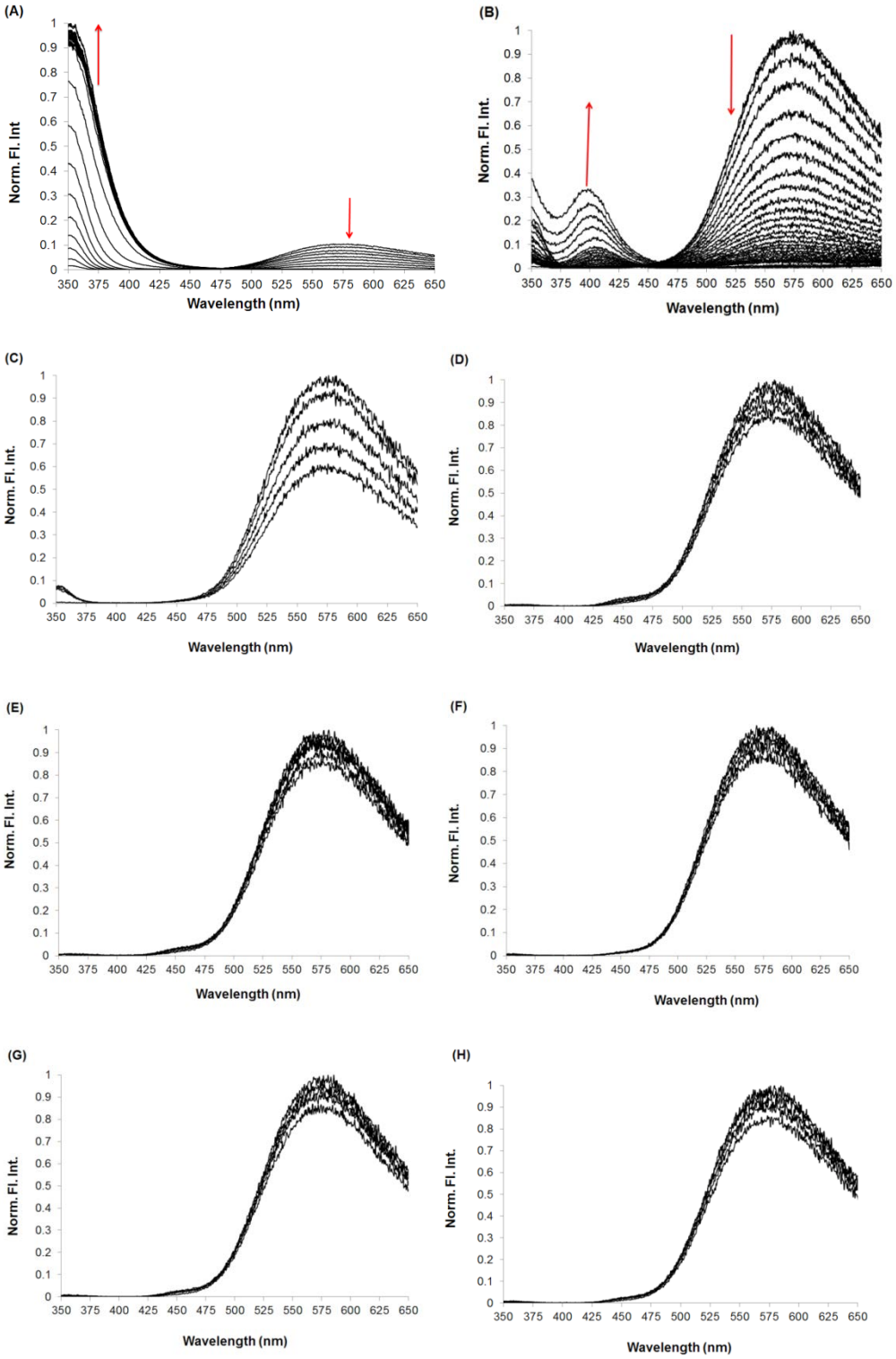
(A)
Norm. Fl. Int
Wavelength (nm)
(B)
Norm. Fl. Int.
Wavelength (nm)
(C)
Norm. Fl. Int.
Wavelength (nm)
(D)
Norm. Fl. Int.
Wavelength (nm)
(E)
Norm. Fl. Int.
Wavelength (nm)
(F)
Norm. Fl. Int.
Wavelength (nm)
(G)
Norm. Fl. Int.
Wavelength (nm)
(H)
Norm. Fl. Int.
Wavelength (nm)

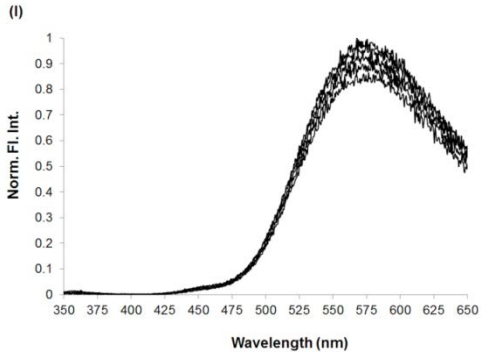
(I)
Norm. Fl. Int.
Wavelength (nm)

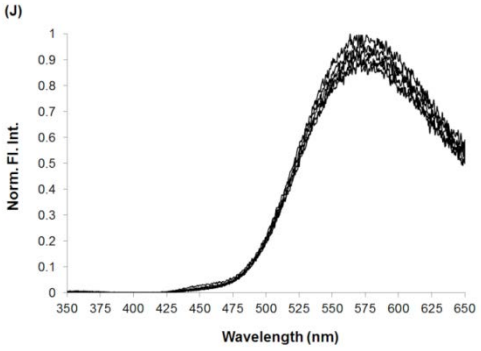
(J)
Norm. Fl. Int.
Wavelength (nm)

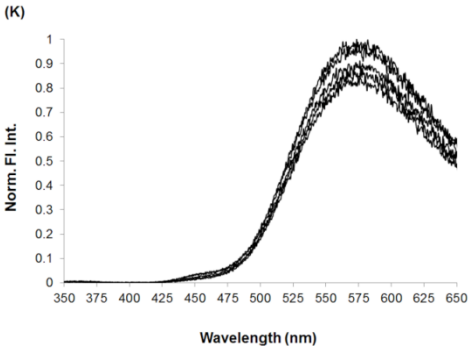
(K)
Norm. Fl. Int.
Wavelength (nm)

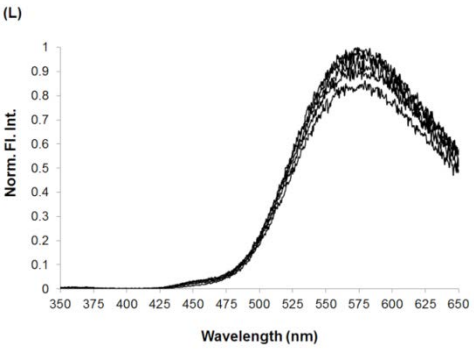
(L)
Norm. Fl. Int.
Wavelength (nm)

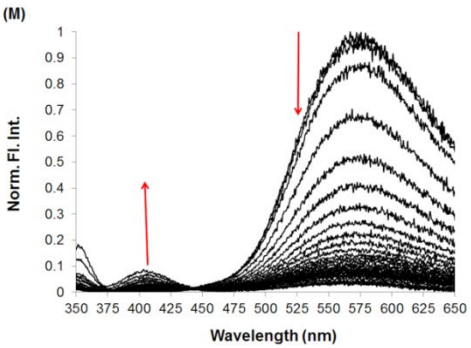
(M)
Norm. Fl. Int.
Wavelength (nm)

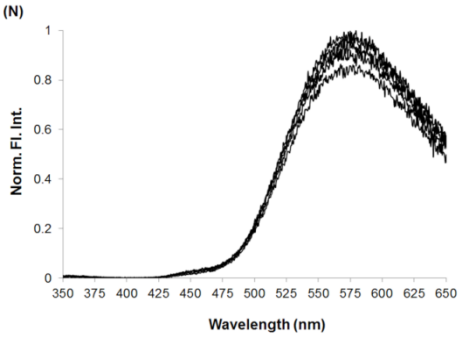
(N)
Norm. Fl. Int.
Wavelength (nm)

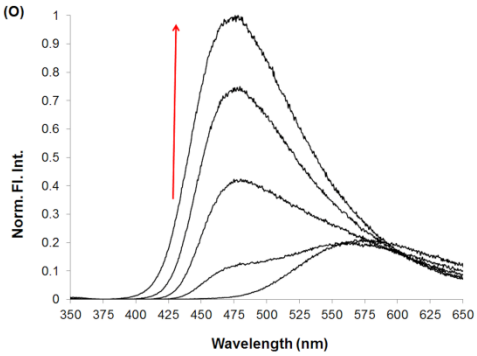
(O)
Norm. Fl. Int.
Wavelength (nm)

Figure S6: Fluorescence response of molecular probe **3** upon the addition of the following anion (16 μmoldm^{-3} in DMSO, λ_{ex} = 339): (A) KCN (B) TBAF (C) $TBAH_2PO_4$ (D) TBABr (E) TBACl (F) TBAI (G) $TBANO_3$ (H) $NaBF_4$ (I) NaN_3 (J) $TBAHSO_4^-$ (K) NH_4SCN (L) $NaClO_4$ (M) $TBACH_3CO_2$ (N) NH_4OH and (O) octylamine.

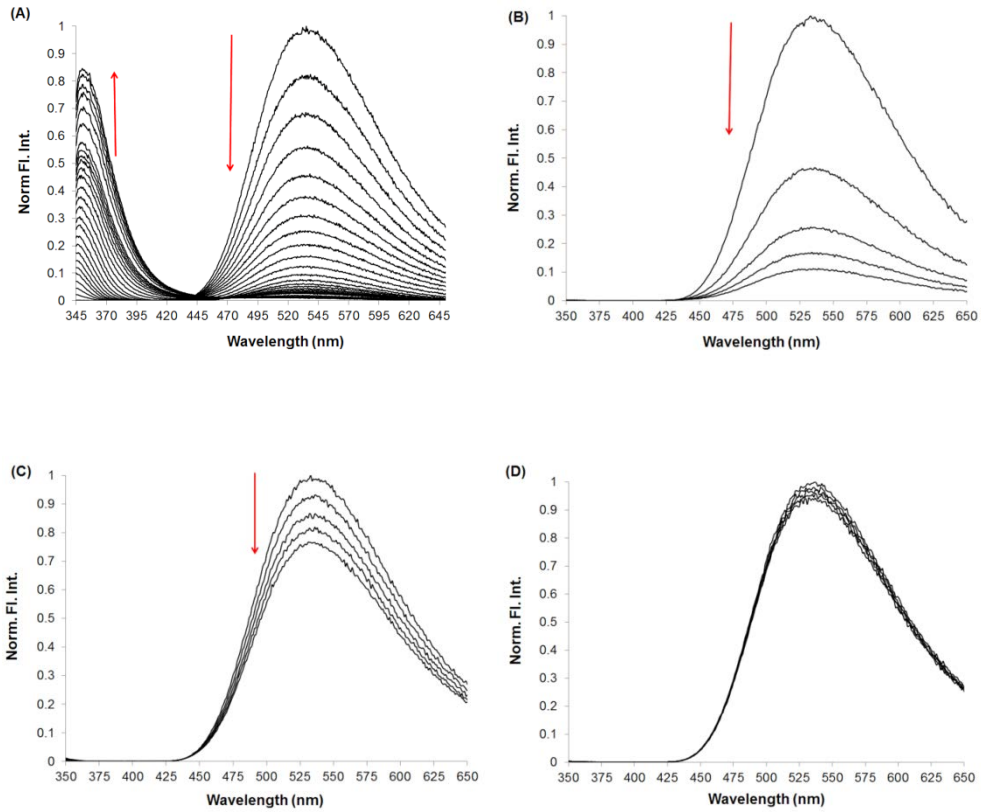

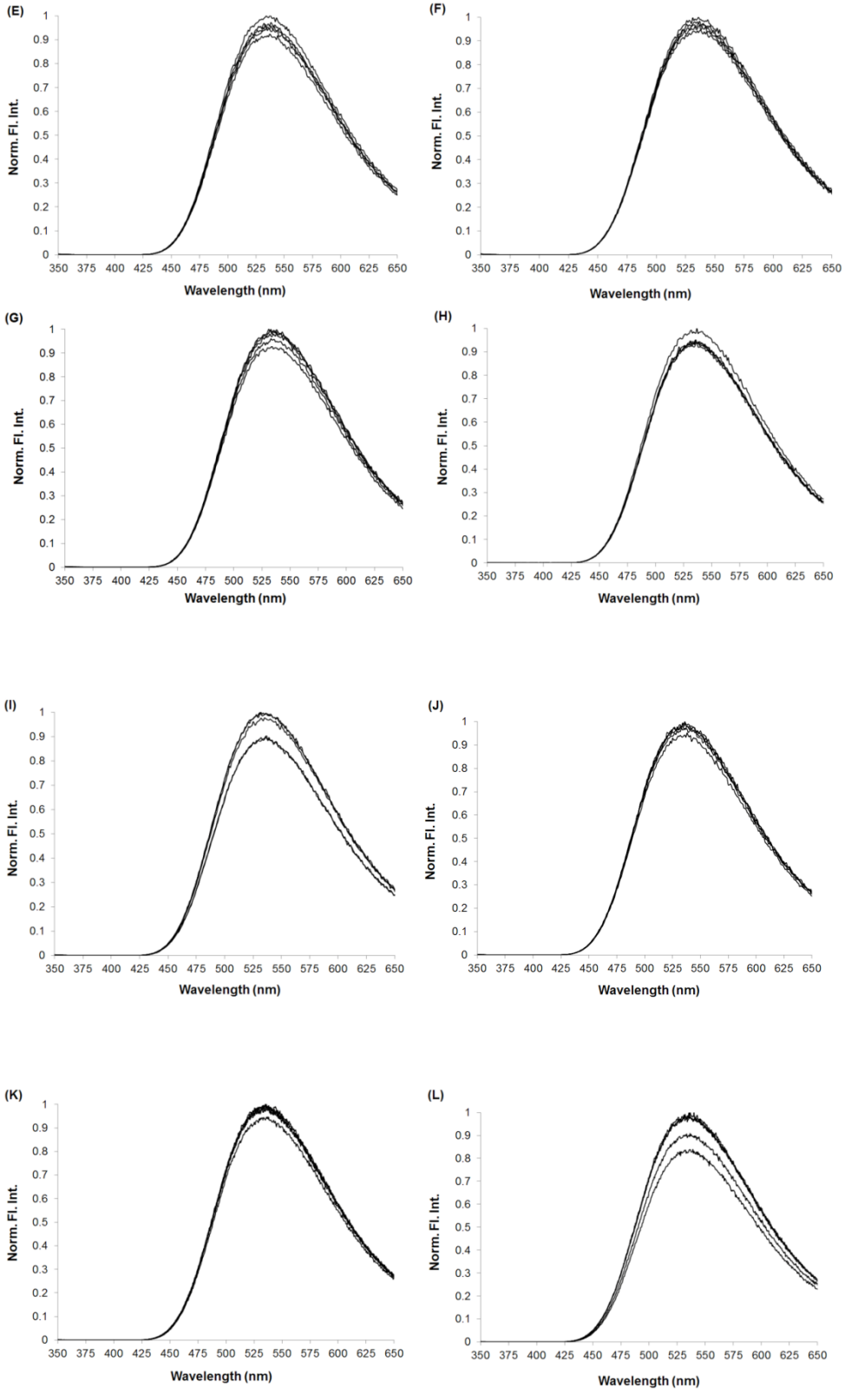
(E)
(F)
(G)
(H)
(I)
(J)
(K)
(L)
Norm. Fl. Int.
Wavelength (nm)
0
0.1
0.2
0.3
0.4
0.5
0.6
0.7
0.8
0.9
1
350 375 400 425 450 475 500 525 550 575 600 625 650

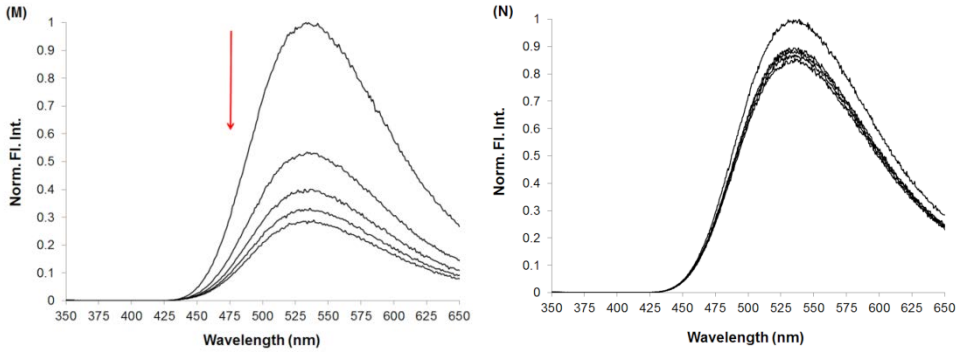

Figure S7: Fluorescence response of molecular probe **4** upon the addition of the following anions in increments of 0.5, 1.0, 1.5 and 2 equivalents of the following anions (16 μmoldm^{-3} in DMSO, λ_{ex} = 339): (A) KCN (B) TBAF (C) $TBAH_2PO_4$ (D) TBABr (E) TBACl (F) TBAI (G) $TBANO_3$ (H) $NaBF_4$ (I) NaN_3 (J) HSO_4^- (K) NH_4SCN (L) NH_4ClO_4 (M) $TBACH_3CO_2$ and (N) NH_4OH.

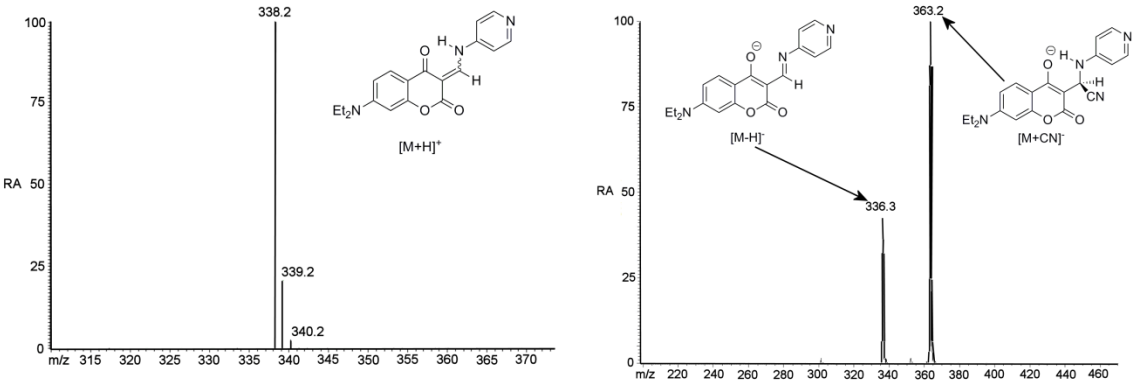

Figure S8: ESI-MS; the free molecular probe (positive mode) and the probe **3**-CN adduct (negative mode). The free molecular probe can also be observed in the negative mode.

NMR studies of probe 3:

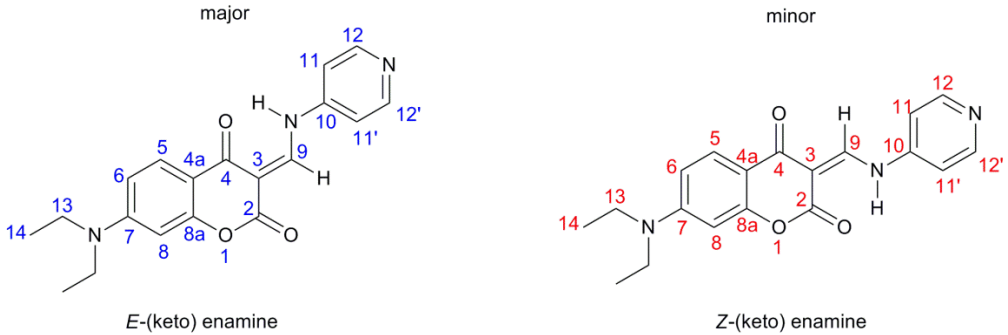

Figure S9: Numbering scheme used for the NMR assignments for molecular probe **3**: the chemical shifts, coupling constants (*J* in Hz) for the two isomers.

	E-(keto)-enamine		*Z*-(keto)-enamine	
Label	proton (ppm, Hz)	carbon (ppm)	proton (ppm, Hz)	carbon (ppm)
2	NA	163.0	NA	164.5
3	NA	99.2	NA	99.7
4	NA	180.2	NA	176.3
4a	NA	152.7	NA	152.6
5	7.84	127.0	7.87	127.5
6	6.58	108.0	6.58	108.0
7	NA	107.7	NA	107.7
8	6.32	96.3	6.34	96.3
8a	NA	156.6	NA	156.3
9	8.85	151.8	8.97	151.8
10	NA	144.4	NA	144.6
11/11’	7.27	111.4	7.32	111.7
12/12’	8.62	150.9	8.62	150.9
13	3.45	44.3	3.45	44.3
14	1.24	11.9	1.24	11.9
-NH	13.47	NA	11.52	NA

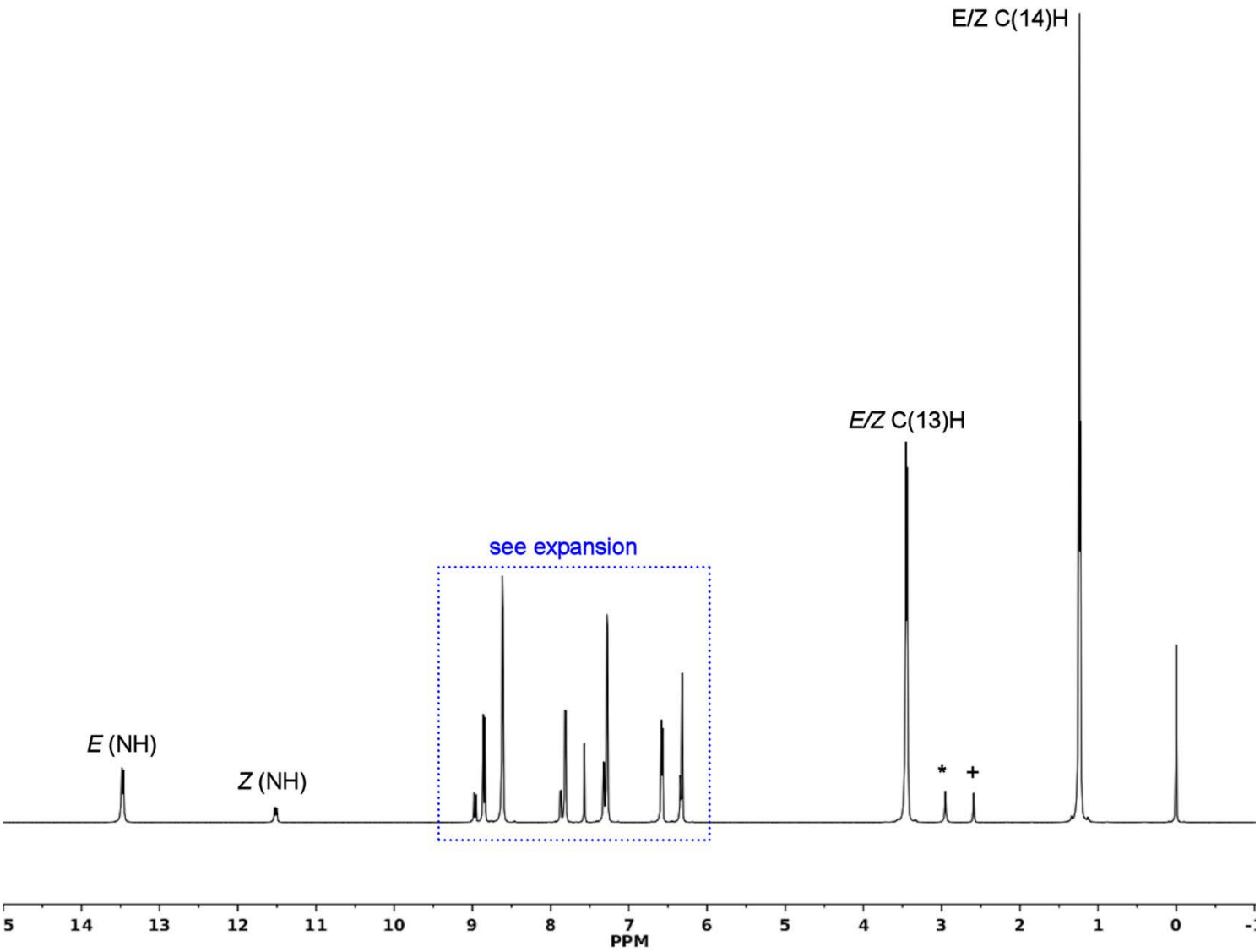

Figure S10: ^{1}H NMR of probe **3** in a mixture of DMSO-d_6:$CHCl_3$-*d* (1:7) (full spectrum).

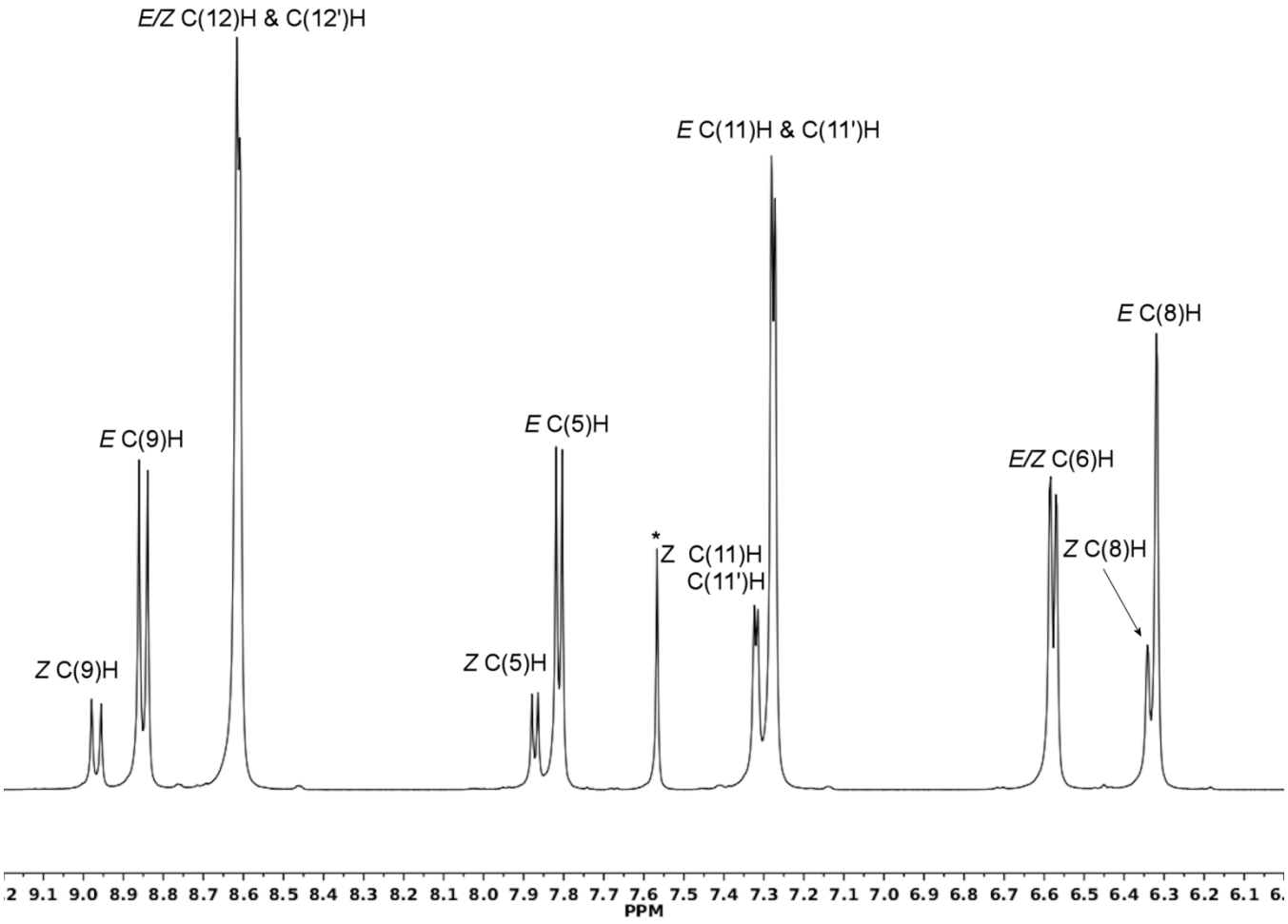

Figure S11: ^{1}H NMR of probe **3** in a mixture of DMSO-d_6:$CHCl_3$-*d* (1:7) (aromatic region).

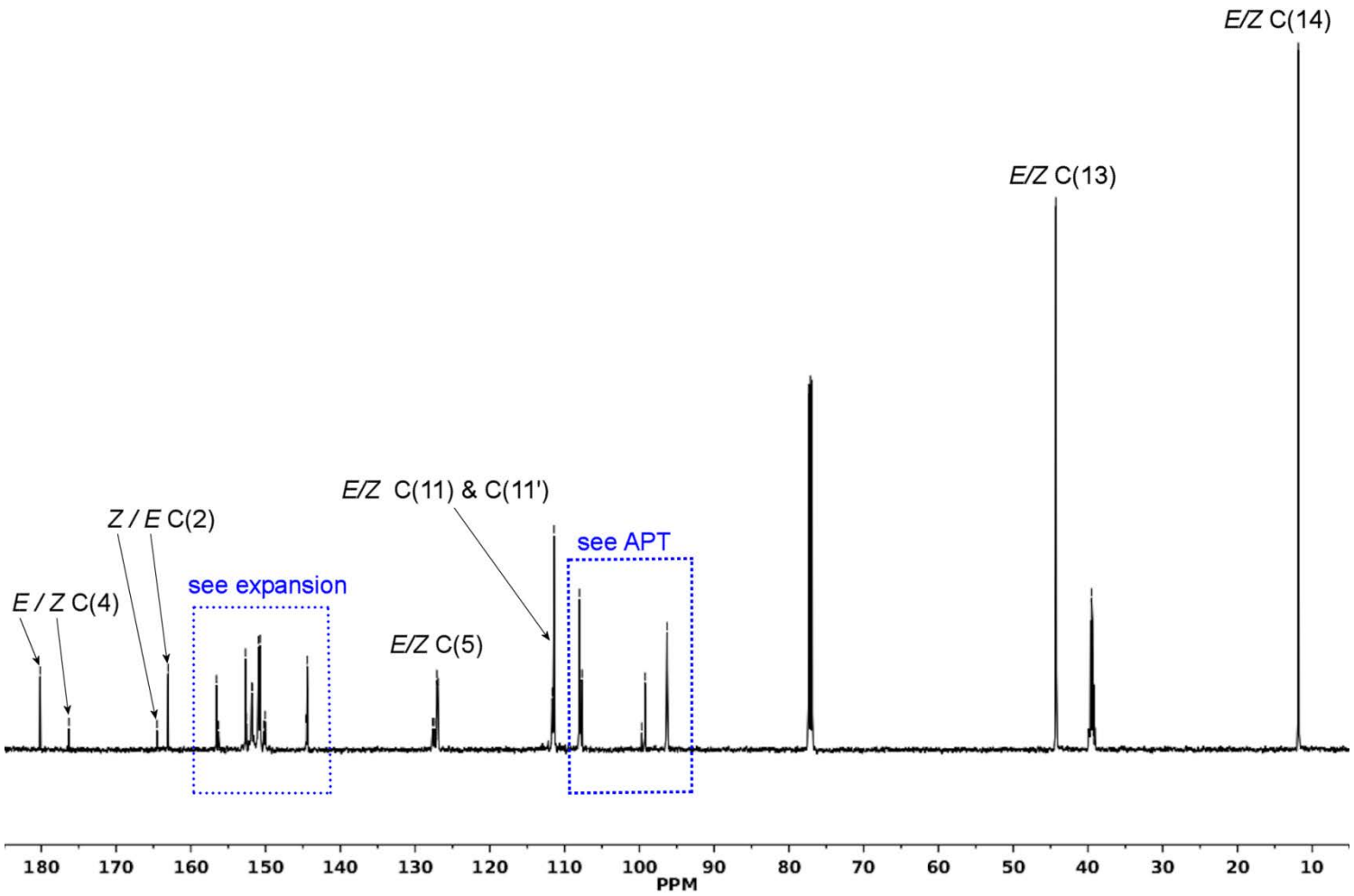

Figure S12: ^{13}C NMR of probe **3** in a mixture of DMSO-d_6:$CHCl_3$-*d* (1:7) (full spectrum).

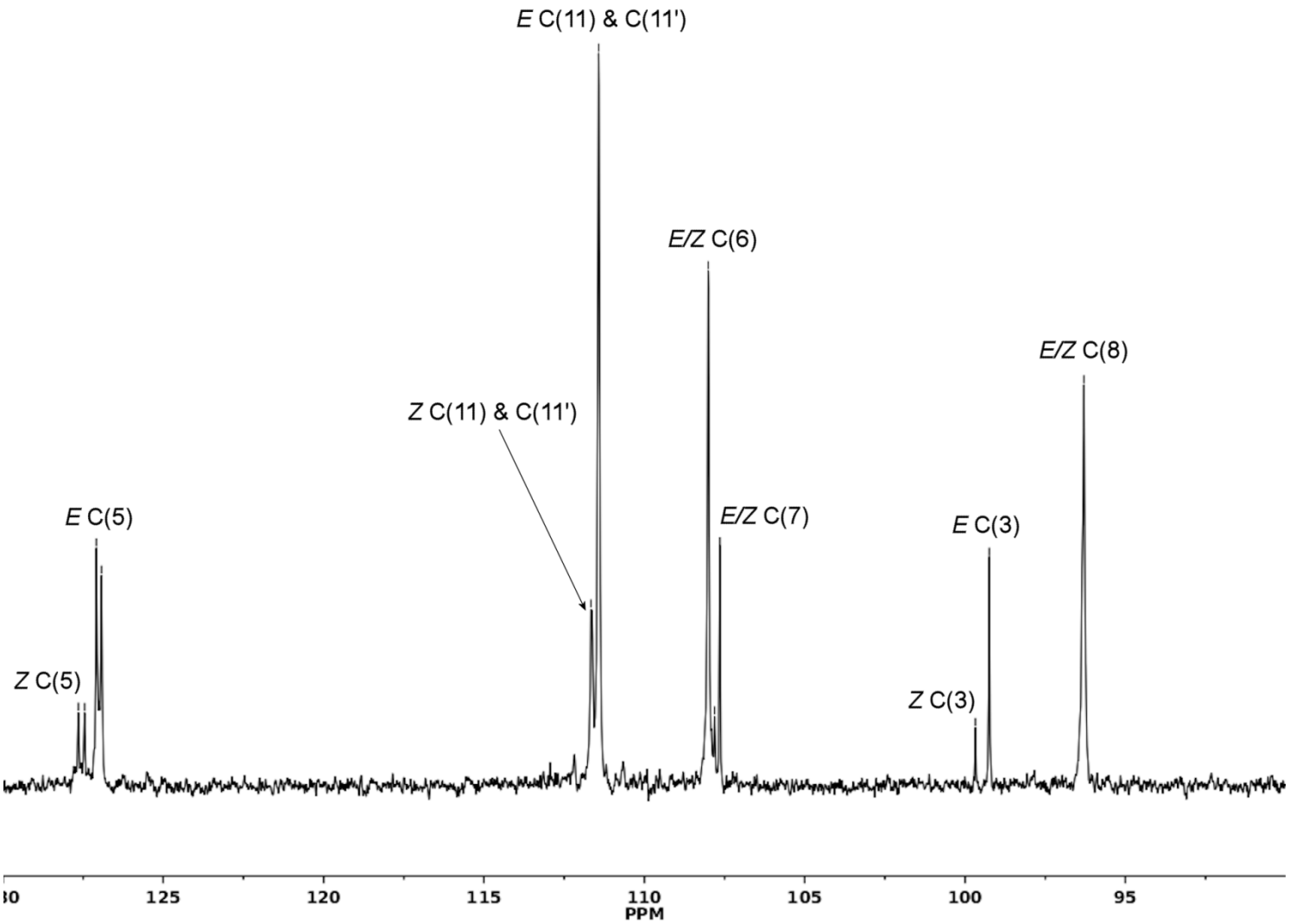

Figure S13: ^{13}C NMR of probe **3** in a mixture of DMSO-d_6:$CHCl_3$-*d* (1:7) (expanded).

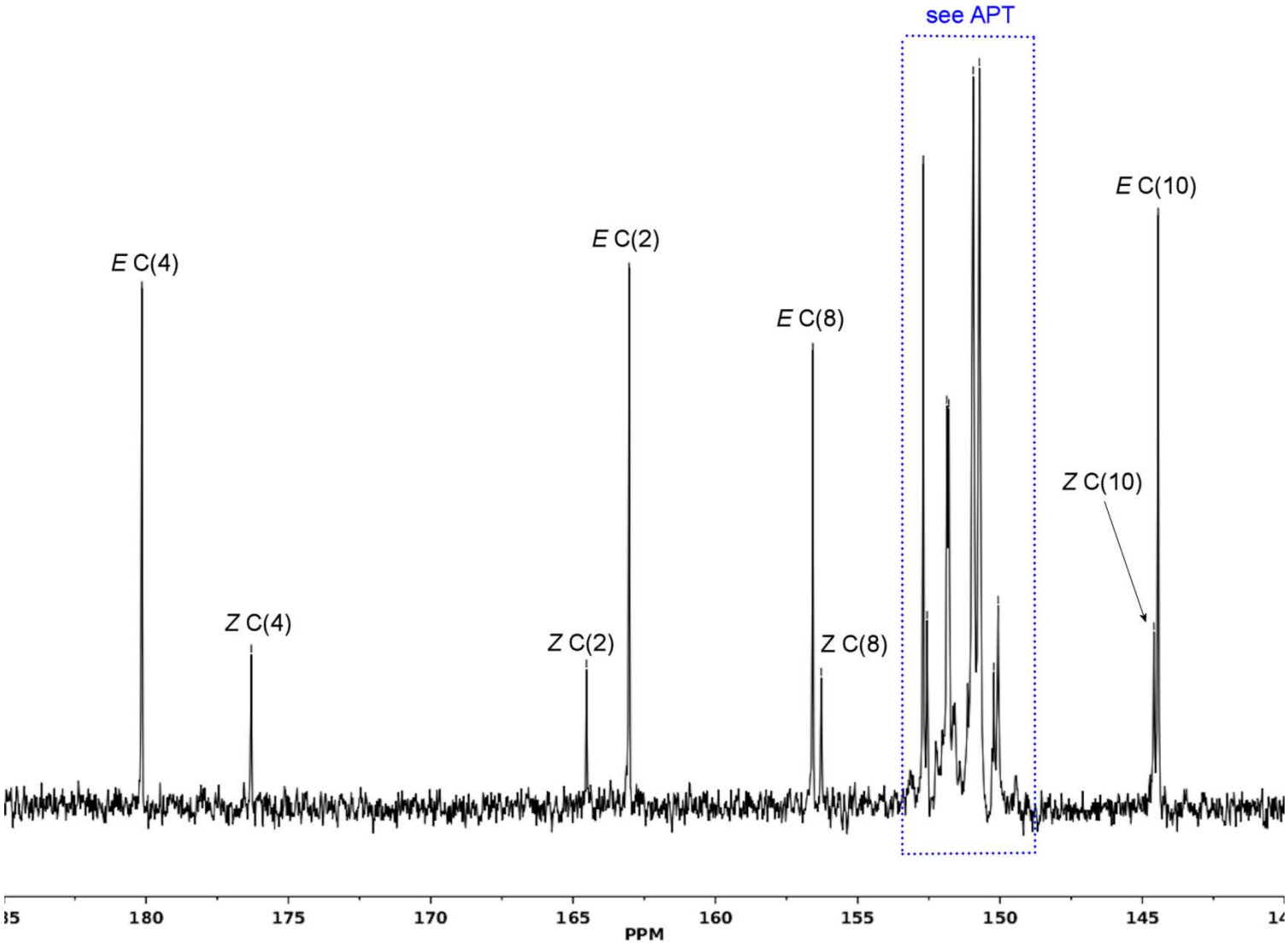

Figure S14: ^{13}C NMR of probe **3** in a mixture of DMSO-d_6:$CHCl_3$-*d* (1:7) (expanded)

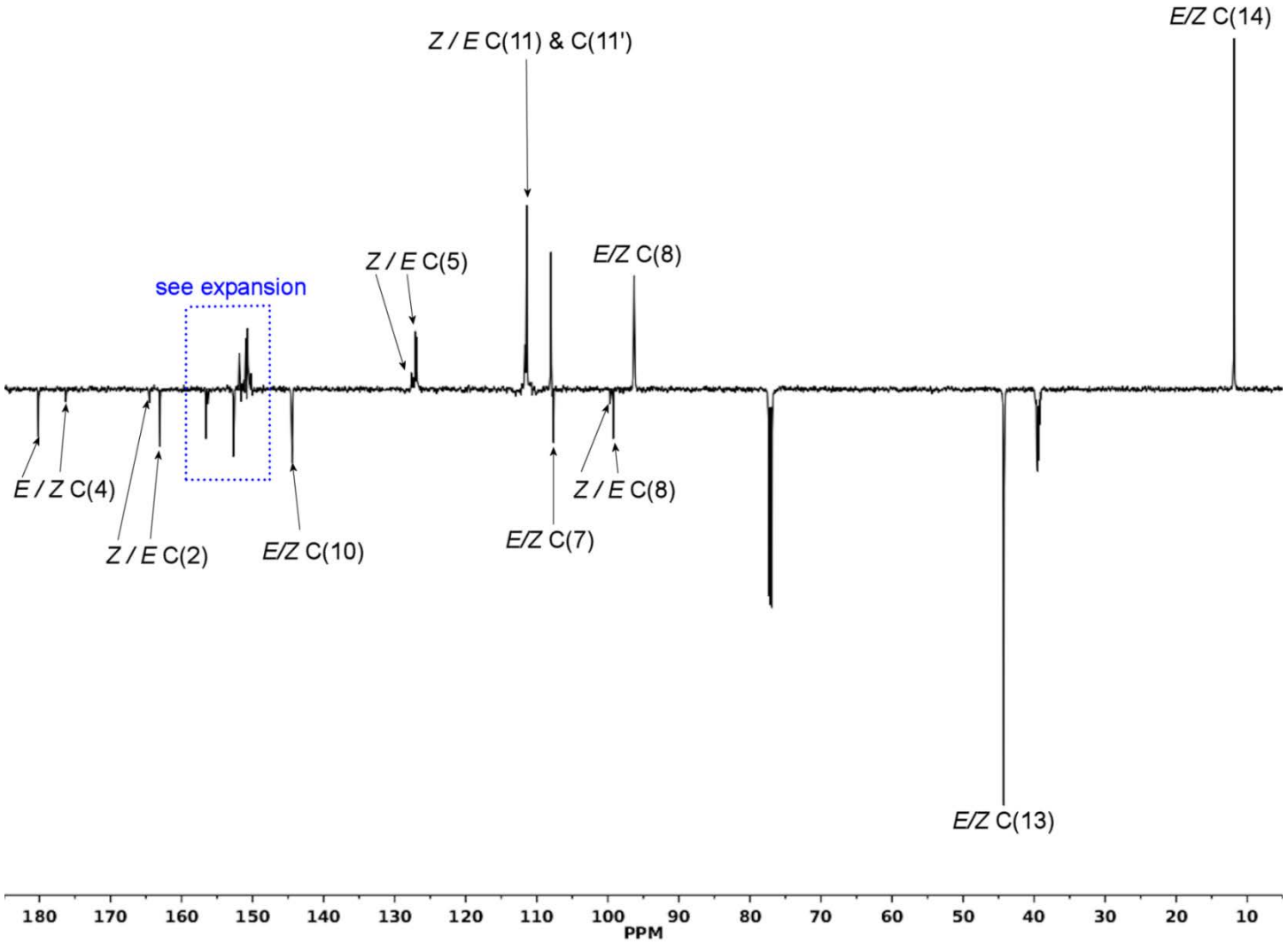

Figure S15: ^{13}C APT of probe **3** in a mixture of DMSO-d_6:$CHCl_3$-*d* (1:7) (full spectrum).

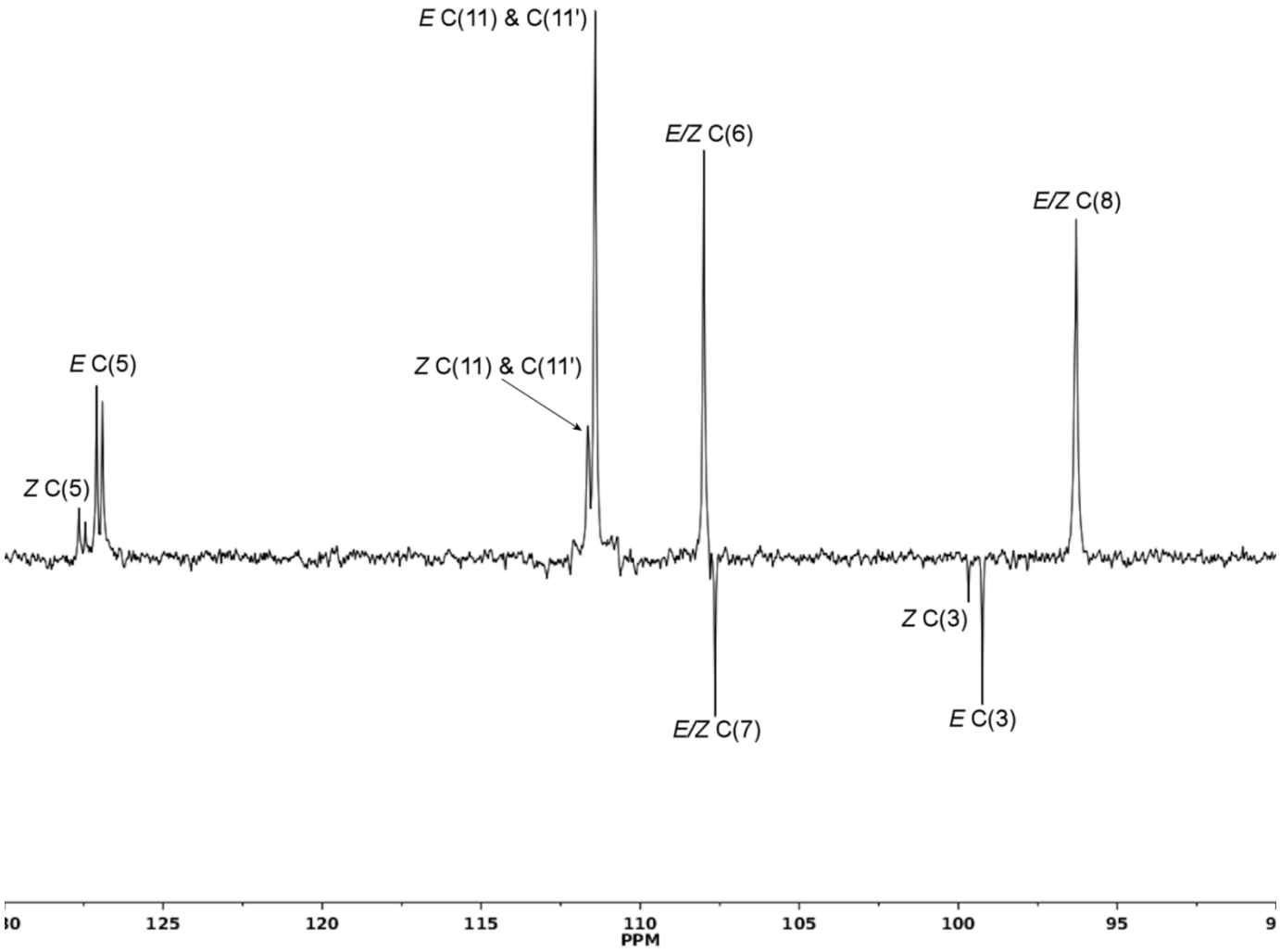

Figure S16: ^{13}C APT of probe **3** in a mixture of DMSO-d_6:$CHCl_3$-*d* (expanded).

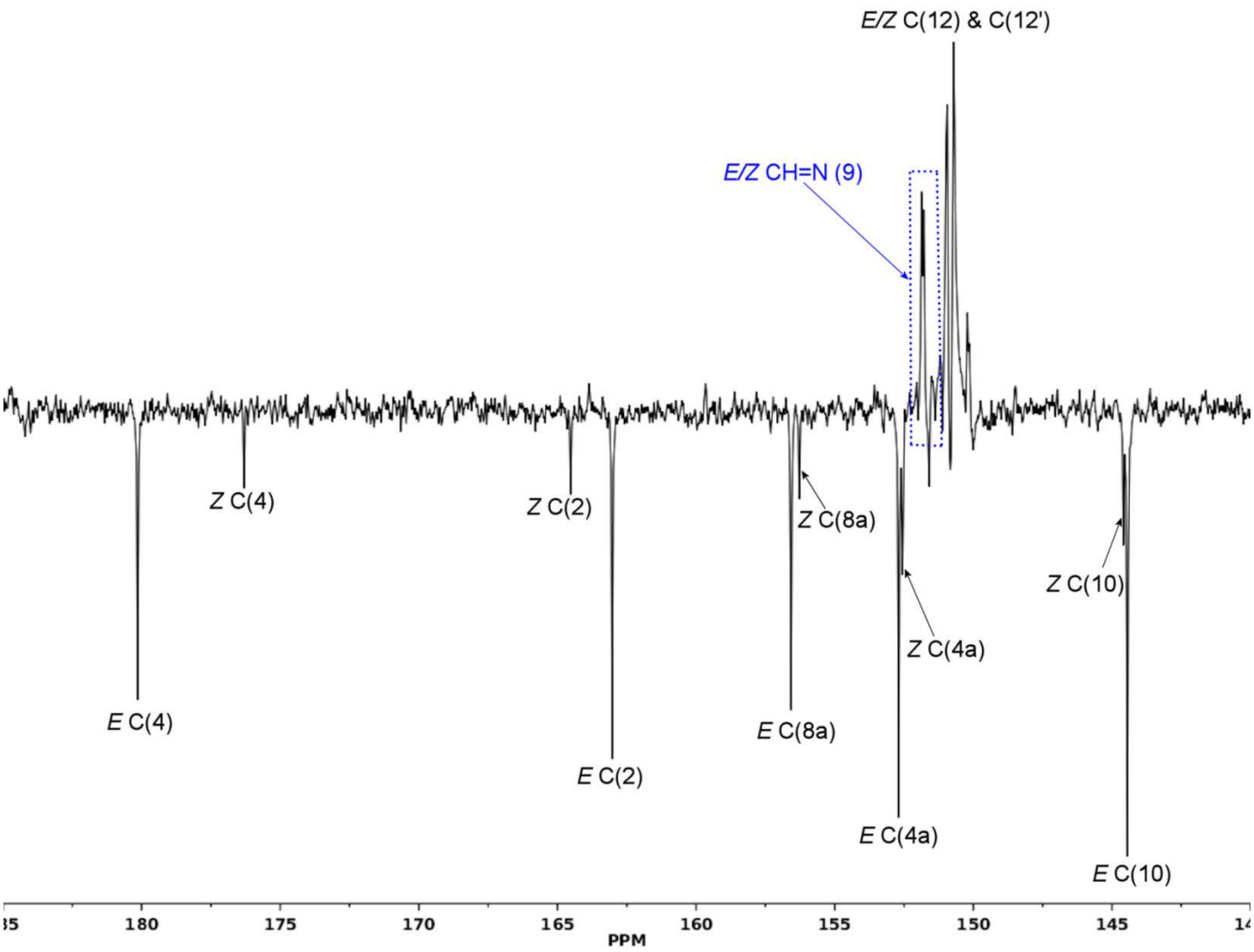

Figure S17: ^{13}C APT of probe **3** in a mixture of DMSO-d_6:$CHCl_3$-*d* (1:7) (expanded).

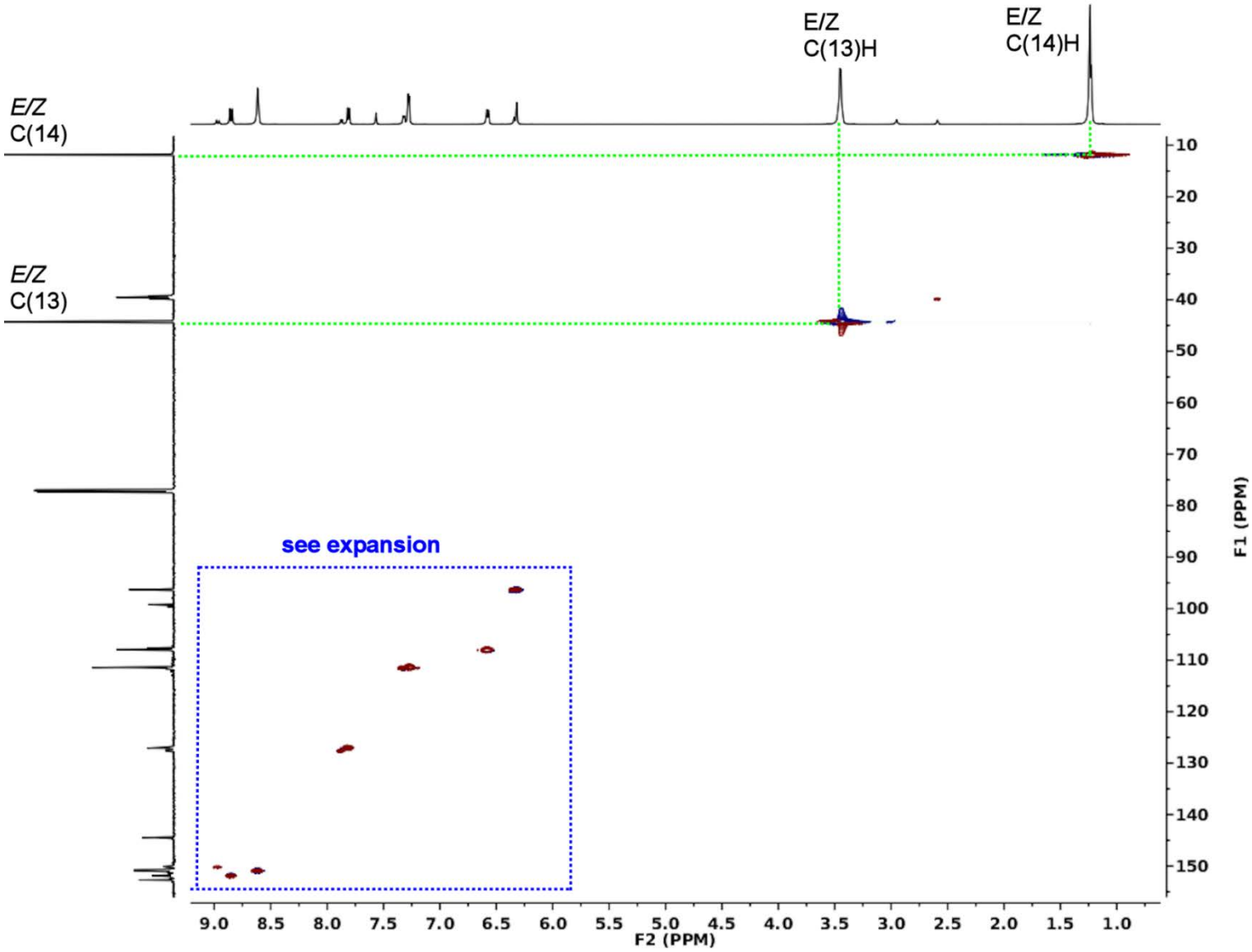

Figure S18: HSQC of probe **3** in a mixture of DMSO-d_6:$CHCl_3$-*d* (1:7).

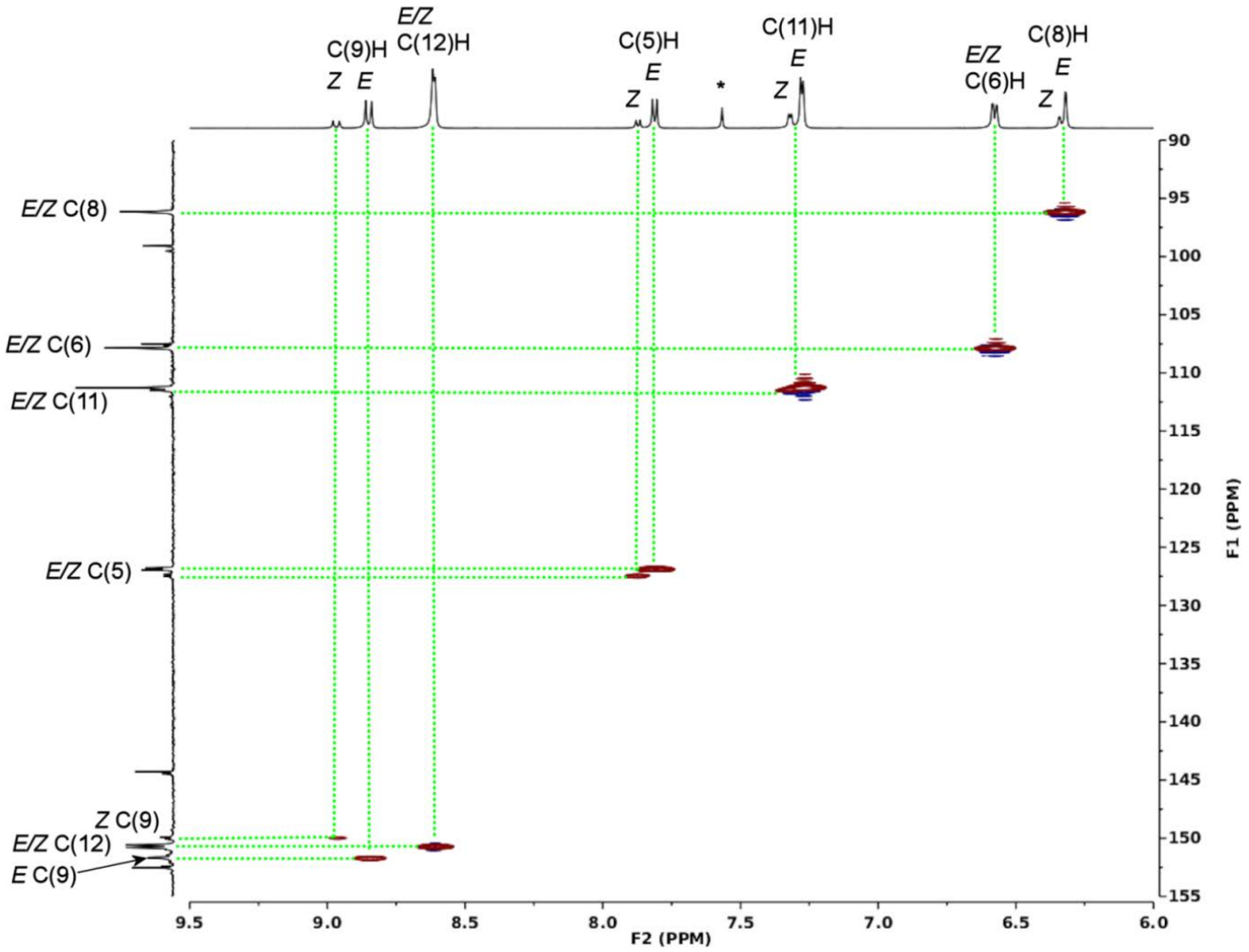

Figure S19: HSQC of probe **3** in a mixture of DMSO-d_6:$CHCl_3$-*d* (full spectrum).

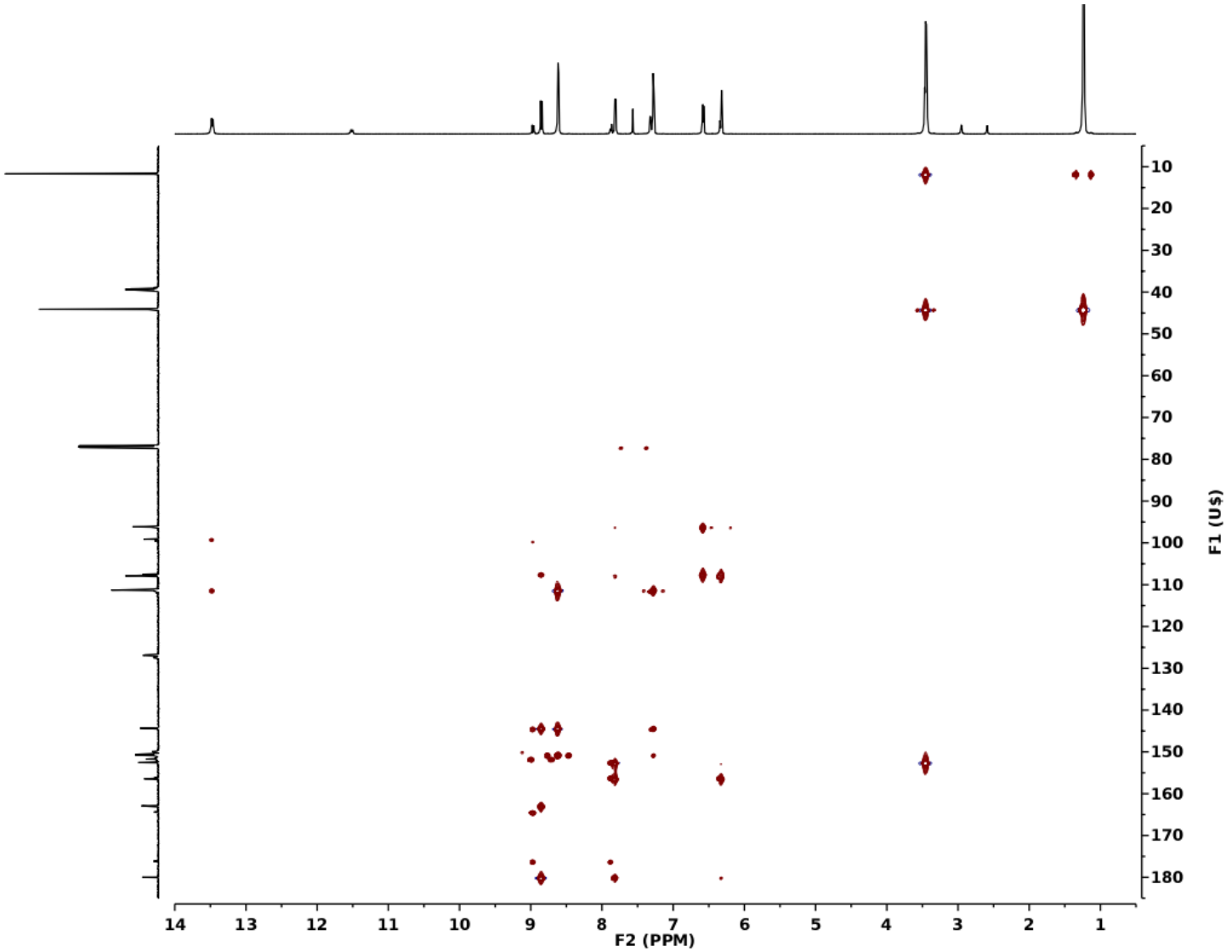

Figure S20: HMBC of probe **3** in a mixture of DMSO-d_6:$CHCl_3$-*d* (full spectrum)

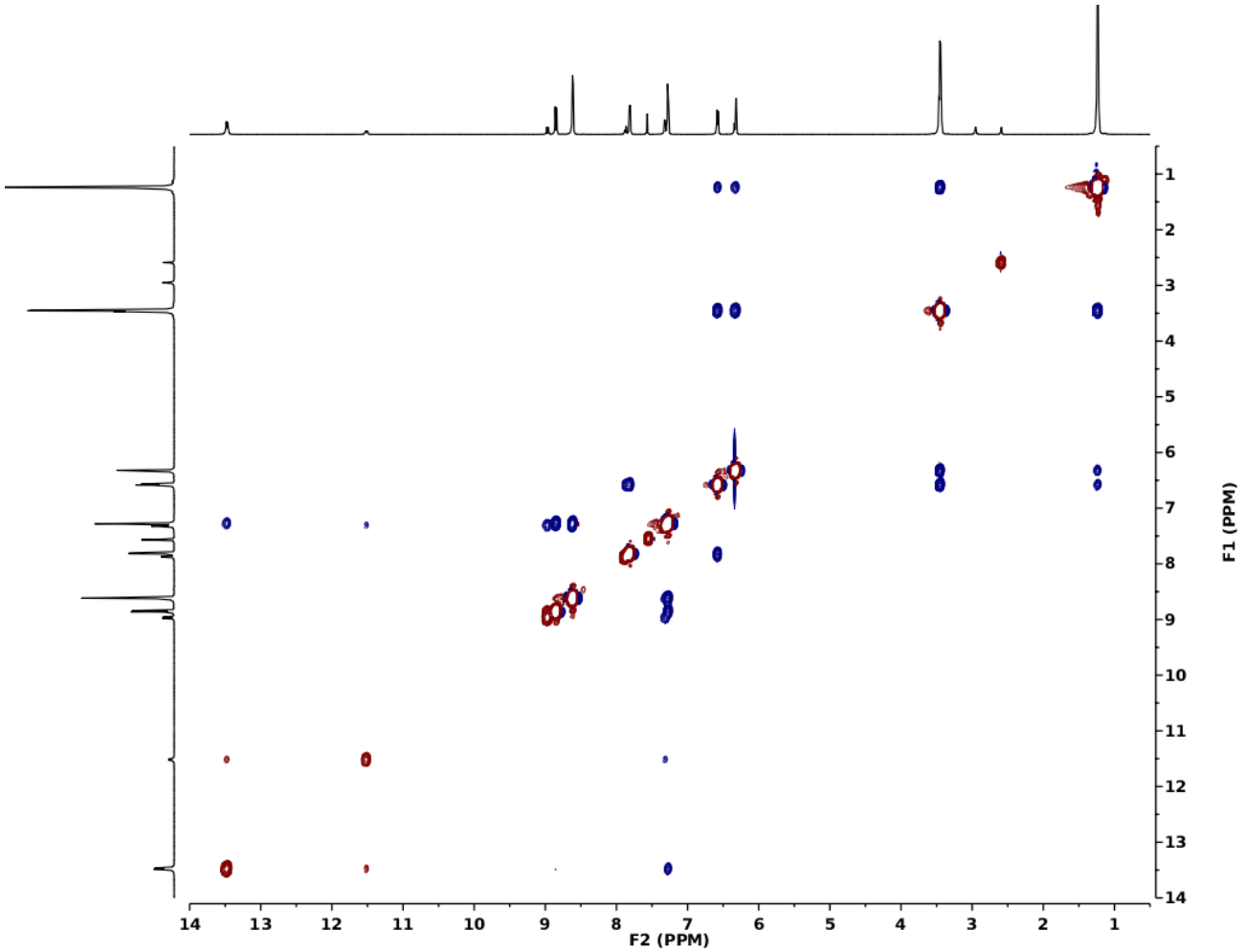

Figure S21: ROESY of probe **3** in a mixture of DMSO-d_6:$CHCl_3$-*d* (full spectrum).

NMR Studies of probe 3-CN adduct:

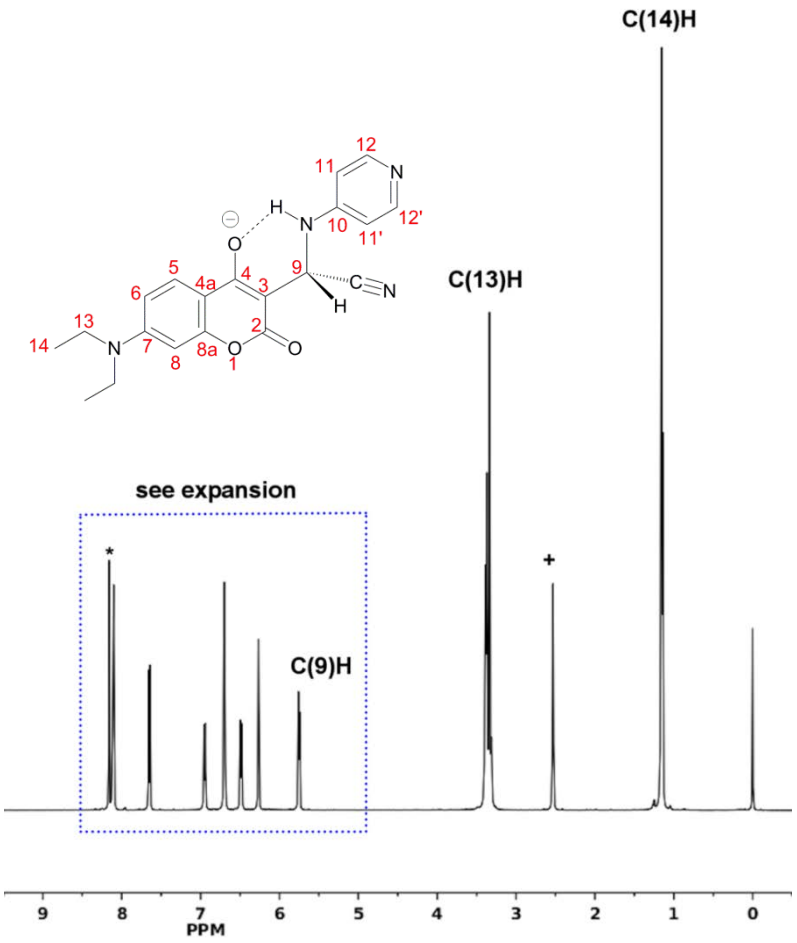

	CN-adduct	
Label	proton (ppm, Hz)	carbon (ppm)
2	NA	163.6
3	NA	88.0
4	NA	173.3
4a	NA	149.3
5	7.65 (1H, *d*, *J* = 8.8 Hz)	125.7
6	6.49 (1H, *d*, *J* = 8.7 Hz)	106.8
7	NA	110.8
8	6.32 (1H, *s*)	96.1
8a	NA	155.4
9	5.75 (1H, *d*, *J* = 8.5 Hz)	125.3
10	NA	151.5
11/11’	6.70 (2H, *d*, *J* = 5.50 Hz)	107.7
12/12’	8.11 (2H, *d*, *J* = 5.6 Hz)	149.1
13	1.15 (4H, *d*, *J* = 7.0 Hz)	43.7
14	1.15 (6H, *t*, J = 7.0 Hz)	12.02
-CN		119.5
-NH	6.95 (1H, d, *J* = 8.8 Hz)	NA

Figure S22: ^{1}H NMR of probe **3** in a mixture of DMSO-d_6:$CHCl_3$-*d* (1.5:1); *Table S5*: the chemical shifts, coupling constants (*J* in Hz) for the cyanide adduct.

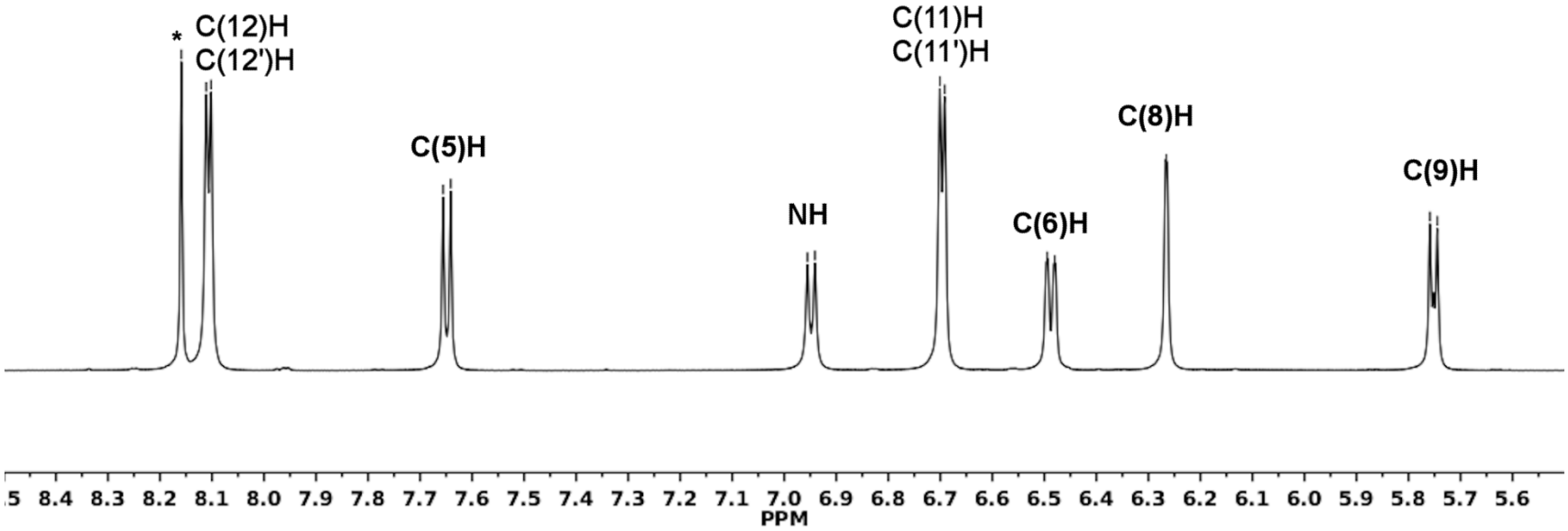

Figure S23: ^{1}H NMR of probe **3** in a mixture of DMSO-d_6:$CHCl_3$-*d* (1.5:1).

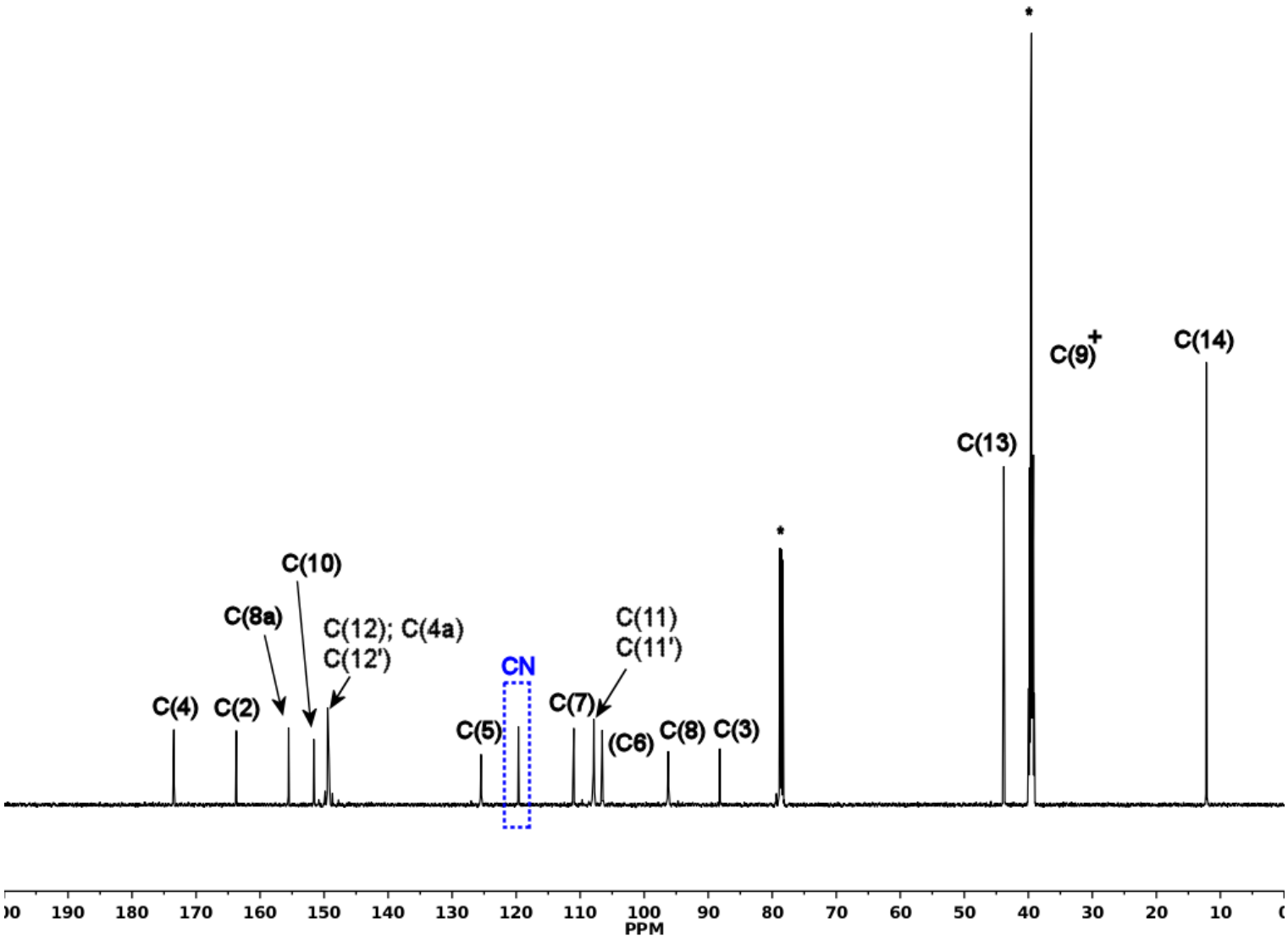

Figure S24: ^{13}C NMR spectrum (full sweep-width) of probe **3** in a mixture of DMSO-d_6:$CHCl_3$-*d* (1.5:1).

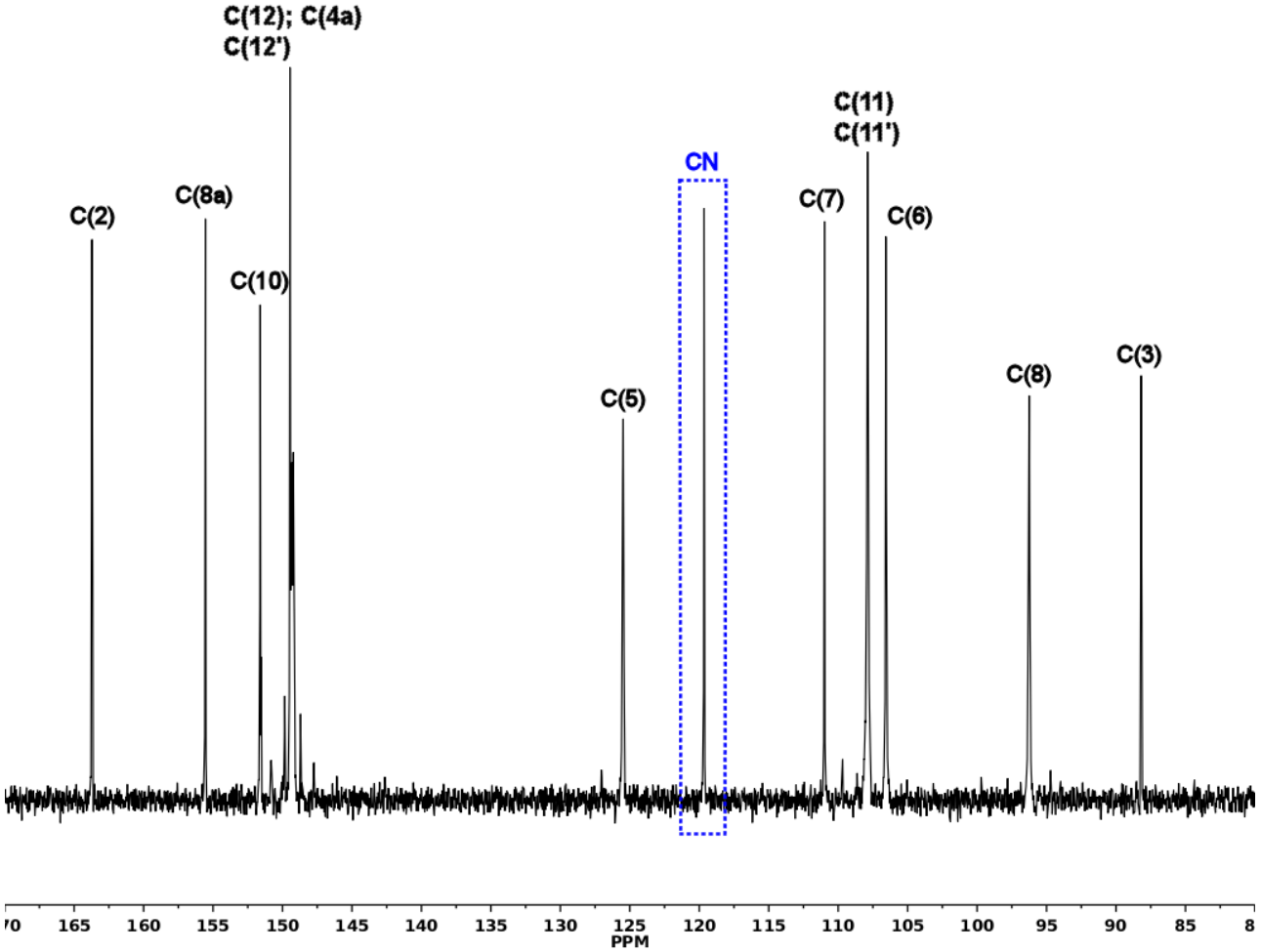

Figure S25: ^{13}C NMR spectrum (expanded) of probe **3** in a mixture of DMSO-d_6:$CHCl_3$-*d* (1.5:1).

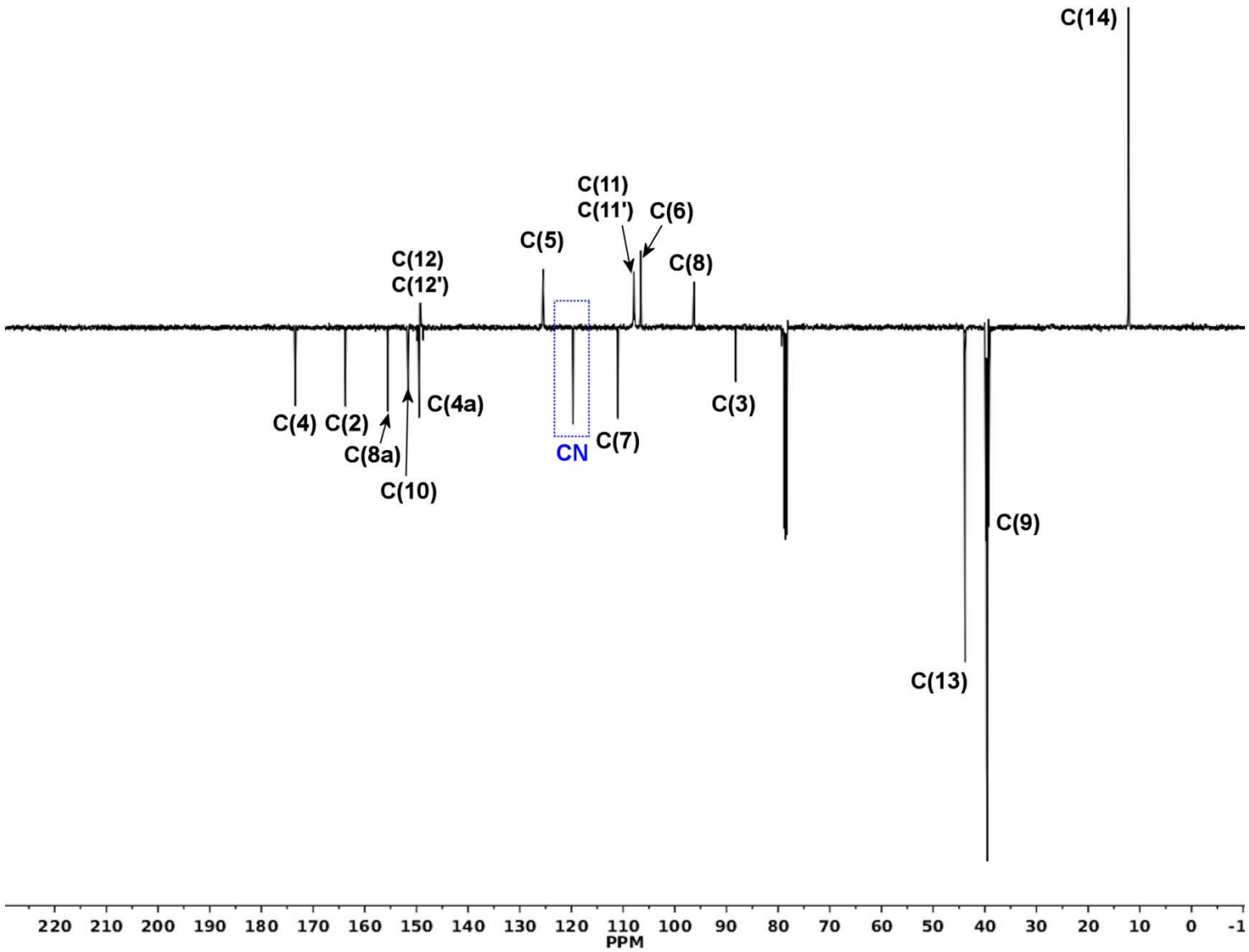

Figure S26: ^{13}C APT spectrum (full sweep-width) of probe **3** in a mixture of DMSO-d_6:$CHCl_3$-*d* (1.5:1).

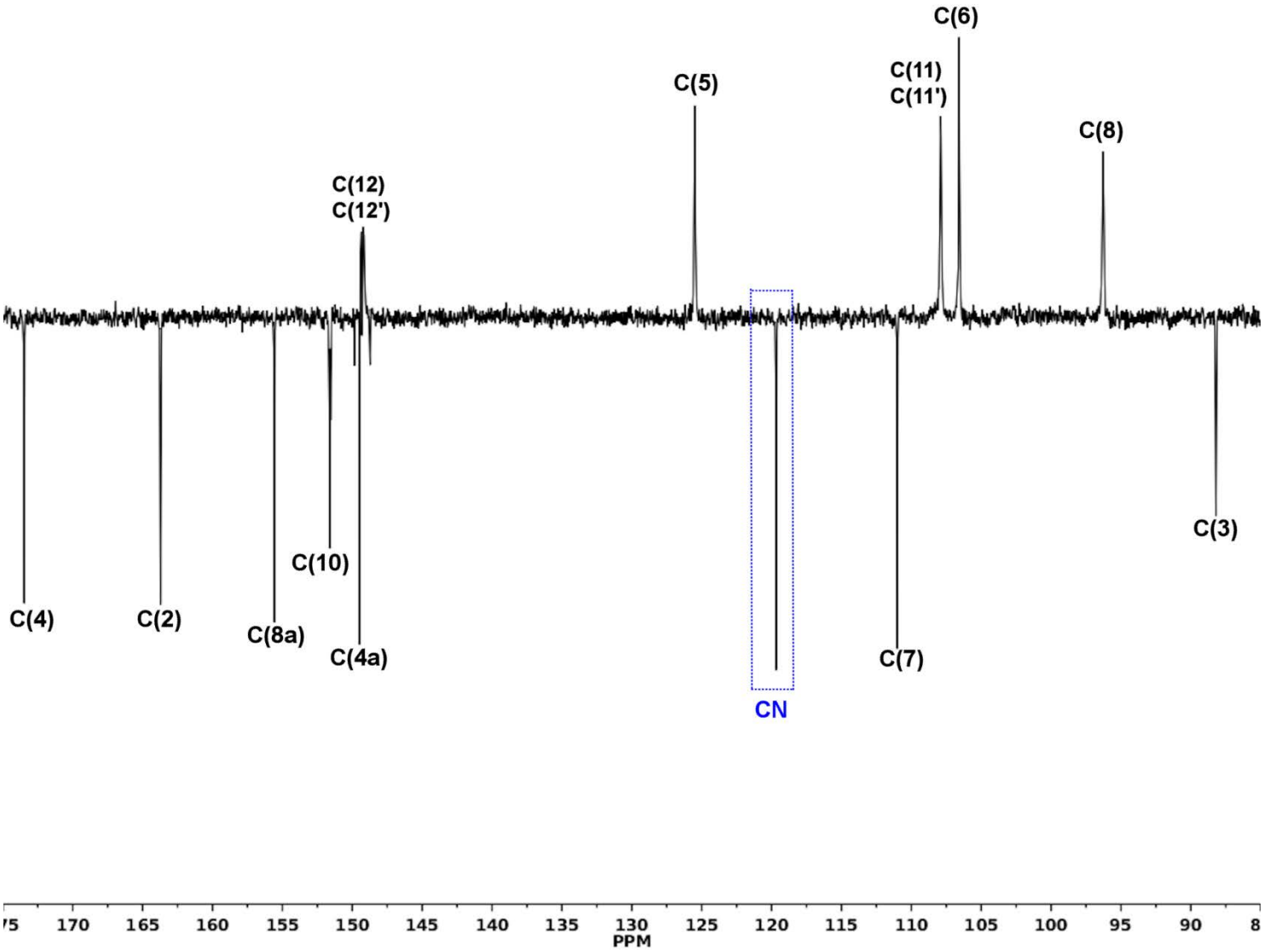

Figure S27: ^{13}C APT spectrum (expanded) of probe **3** in a mixture of DMSO-d_6:$CHCl_3$-*d* (1.5:1).

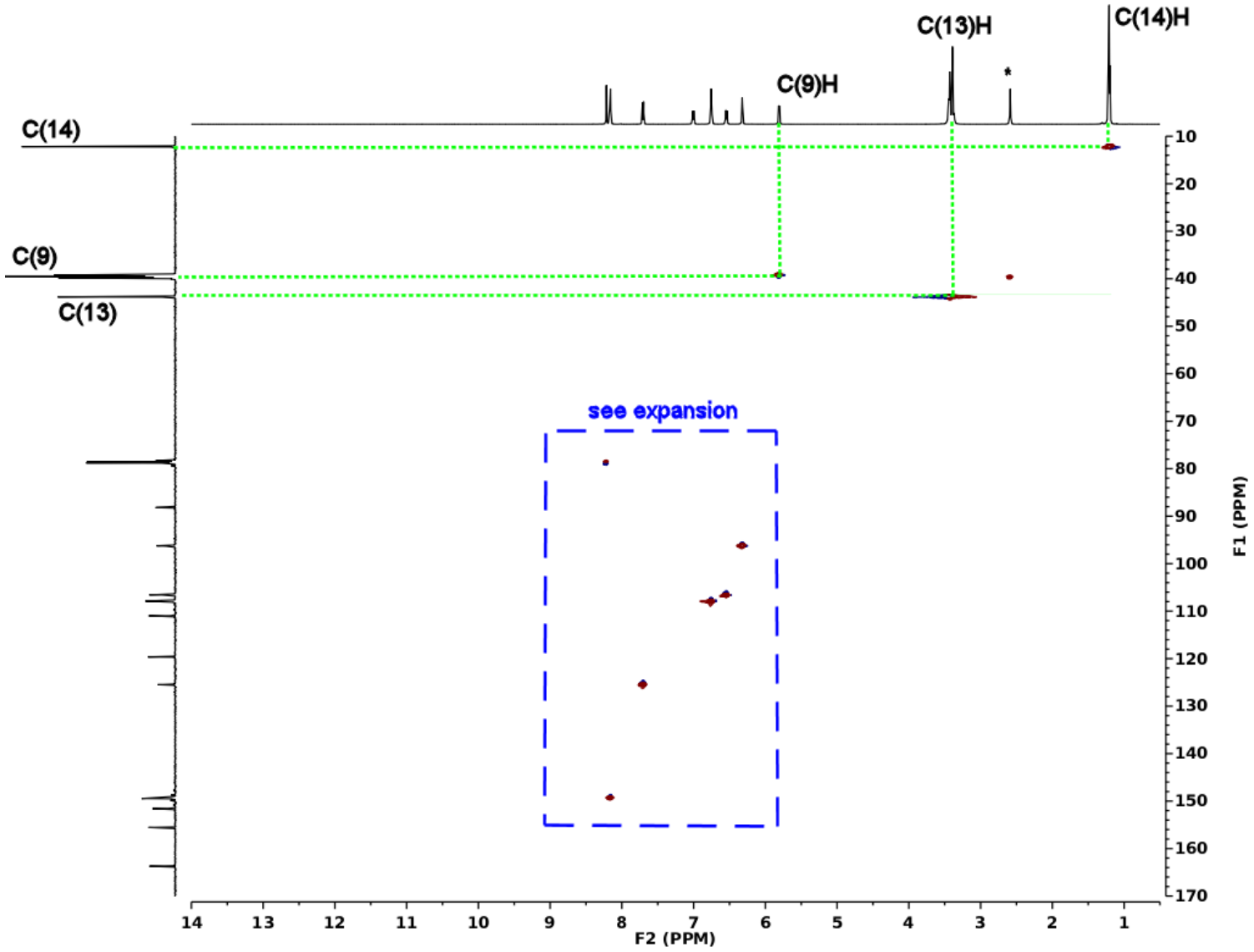

Figure S28: HSQC spectrum (full sweep-width) of probe **3** in a mixture of DMSO-d_6:$CHCl_3$-*d* (1.5:1).

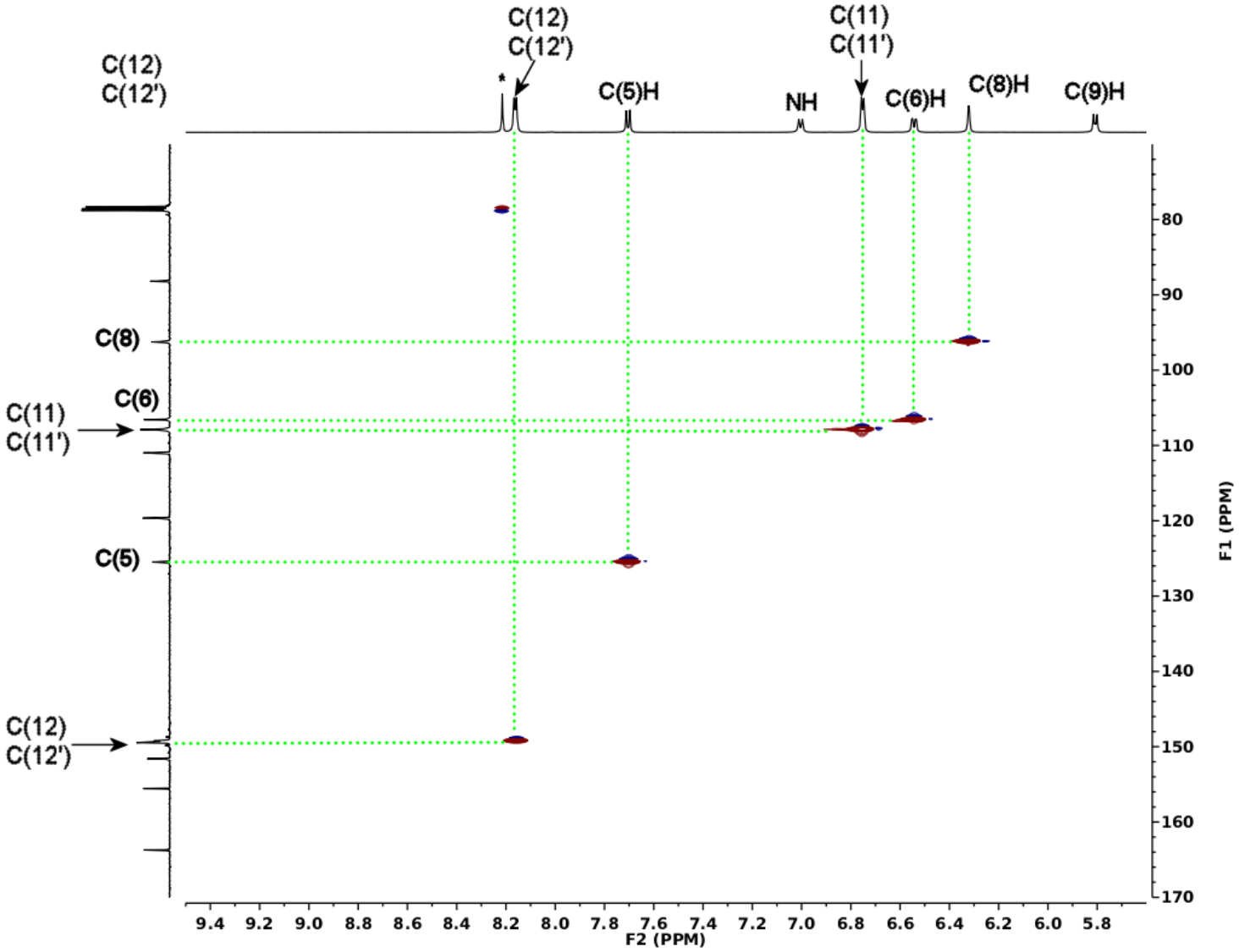

Figure S29: HSQC spectrum (expanded) of probe **3** in a mixture of DMSO-d_6:$CHCl_3$-*d* (1.5:1).

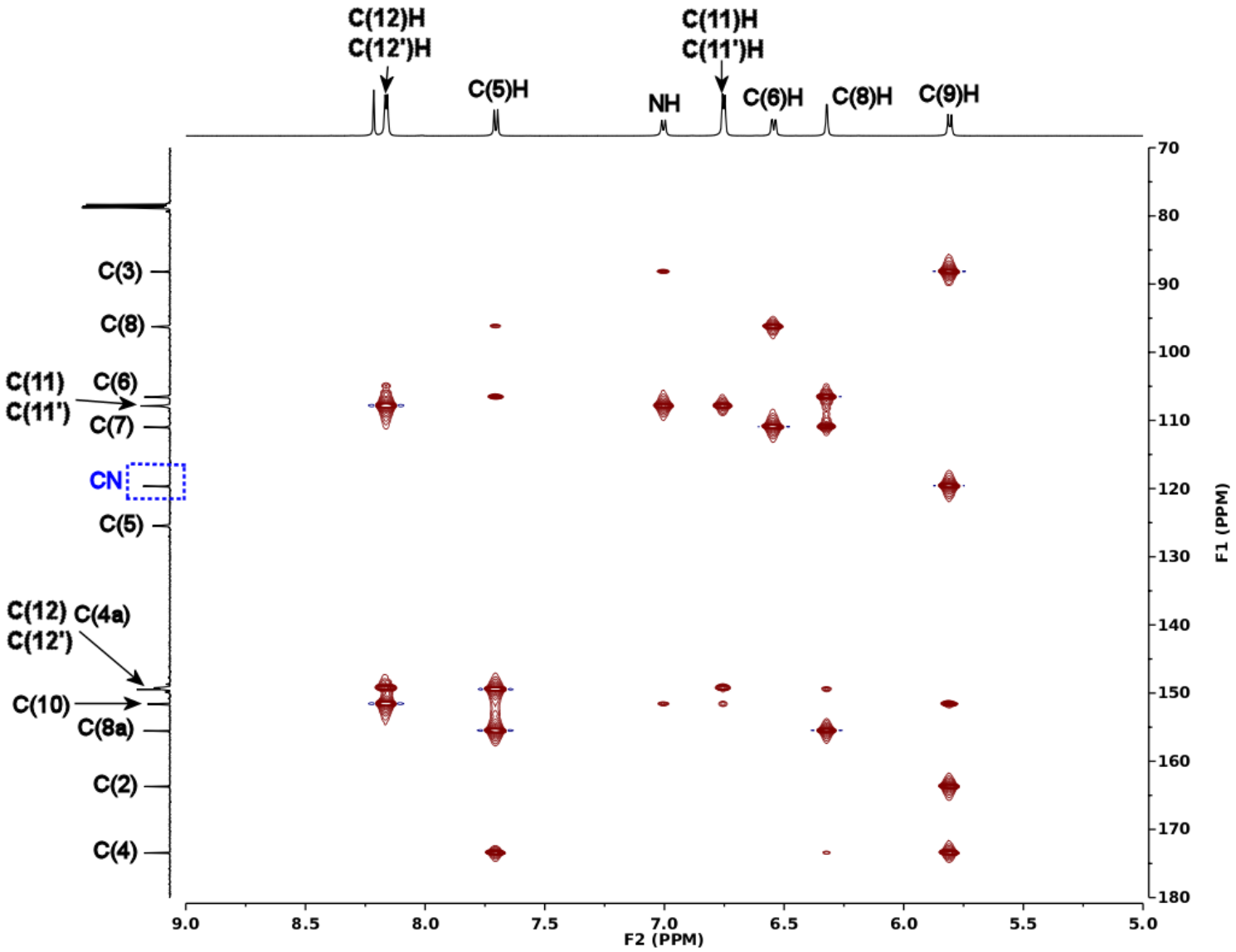

Figure S30: HMBC spectrum (expanded) of probe **3** in a mixture of DMSO-d_6:$CHCl_3$-*d* (1.5:1).

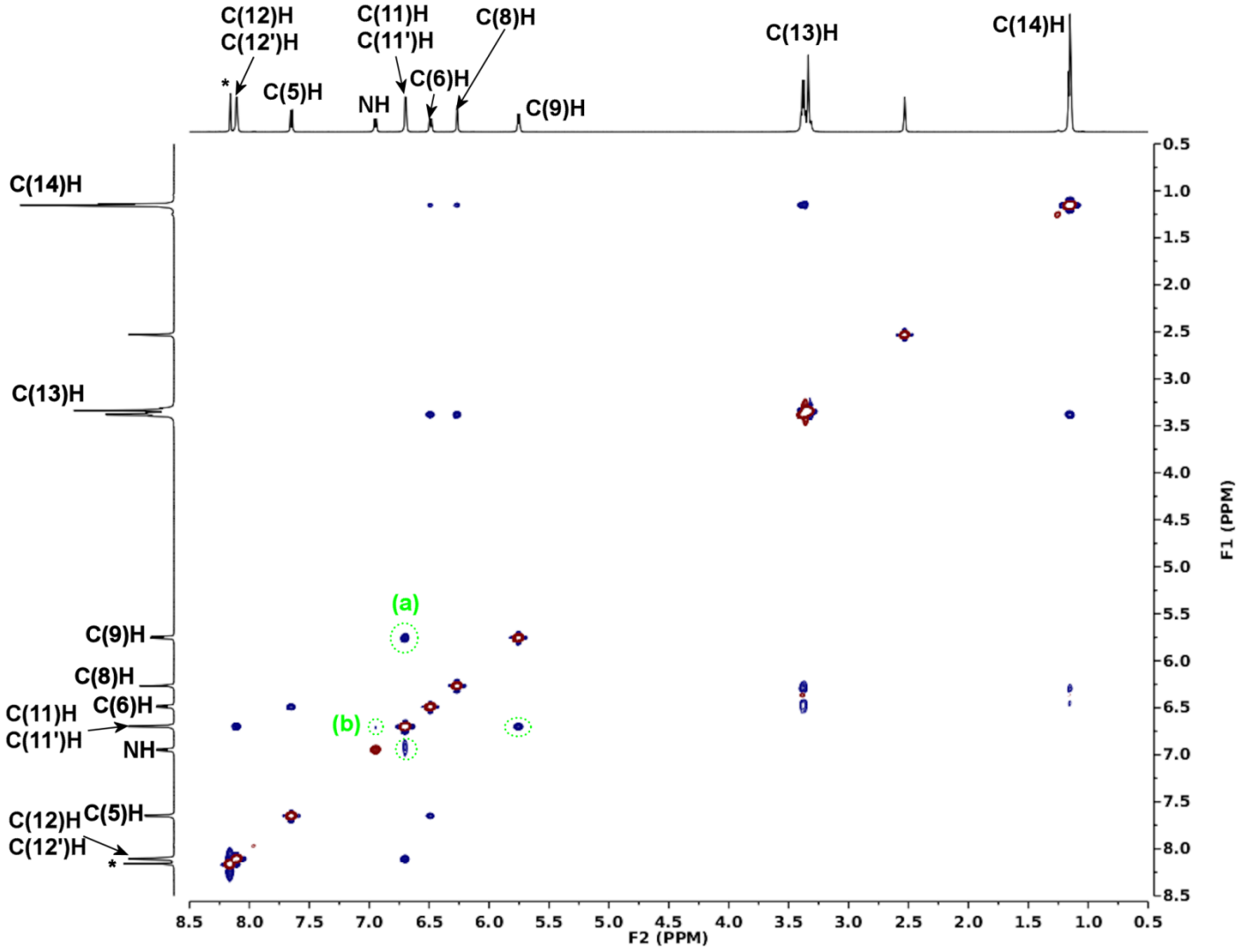

Figure S31: ROESY spectrum (full sweep-width) of probe **3** in a mixture of DMSO-d_6:$CHCl_3$-*d* (1.5:1).

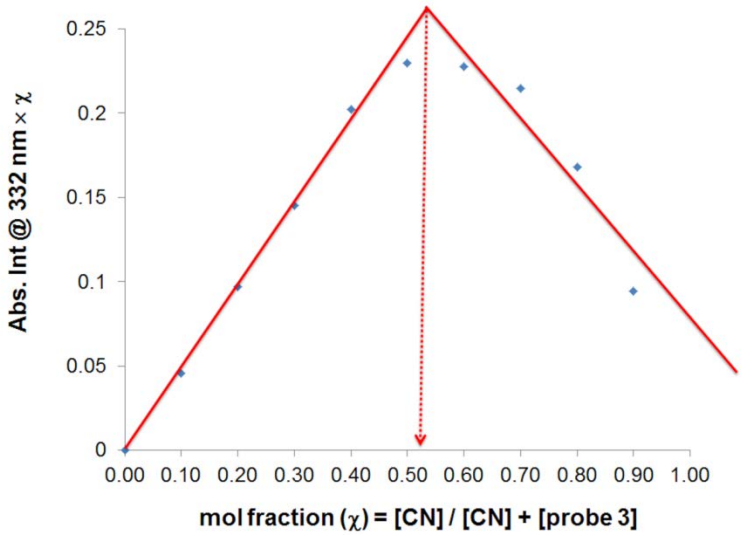

Figure S32: Job's plot showing a 1:1 adduct.

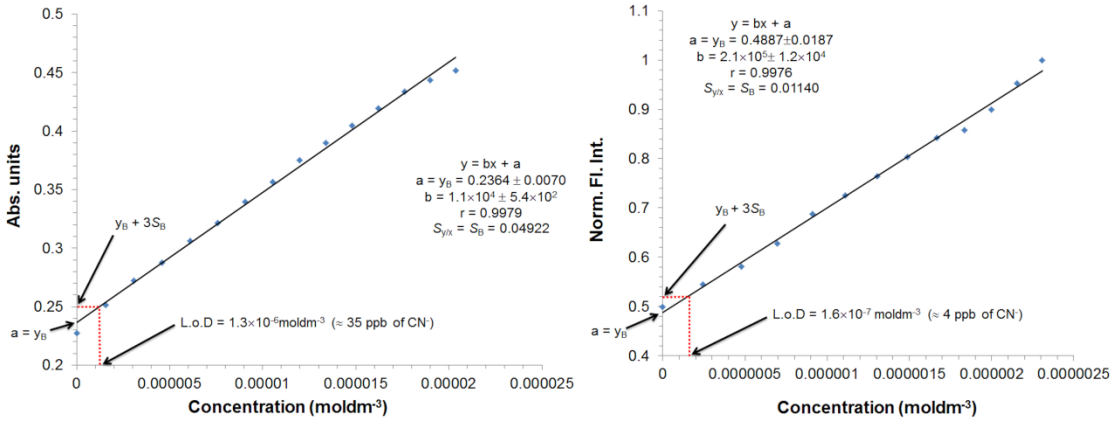

Figure S33: Calibration curve used to calculate the limit of detection CN- using UV-Vis (left) and fluorescence (right) spectroscopy of probe **3**.

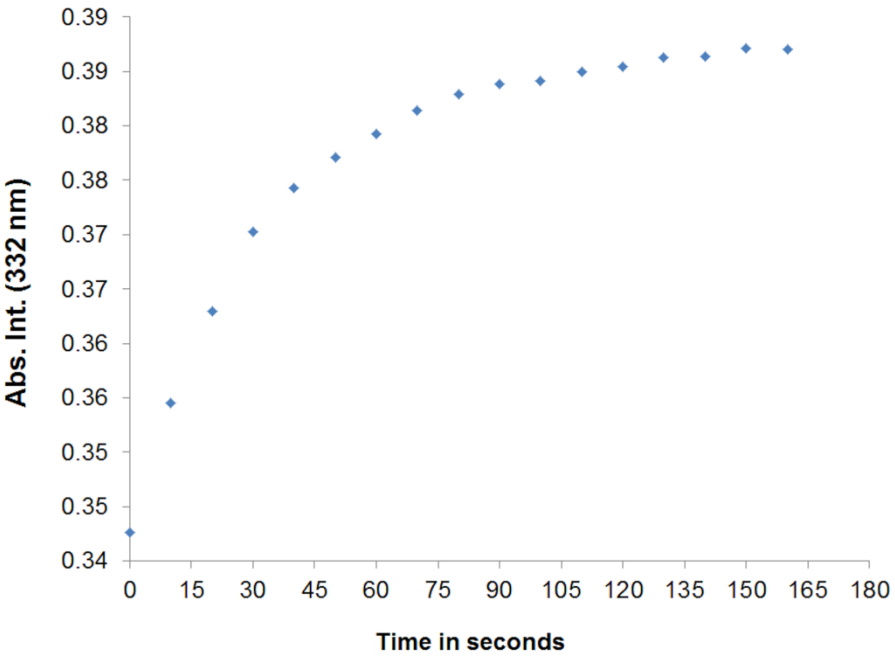

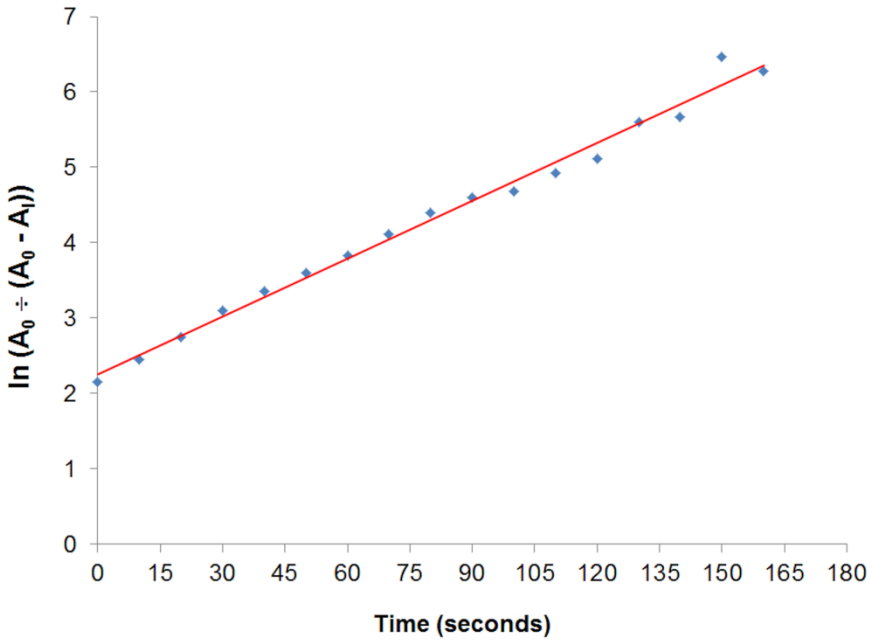

Figure S34: (Top) Absorbance intensity increase upon the cyanide addition to molecular probe **3**, (Bottom) pseudo-first order kinetic plot ln (A_0/(A_0-A_i))

Molecular Modelling

Experimental

Computational methods: Structure **A** was constructed using the 'Build' option in *Spartan '14* [2] installed on a desktop computer equipped with Intel Xenon Dual Quad Core CPUs running at 2.33 GHz. Analysis of 144 conformers resulted in two groups being retained: a cluster of 14 very similar structures within 7.6 $kJmol^{-1}$ of the lowest energy conformer a second cluster of 17 structures related to structure **B** with energies between 58.7 $kJmol^{-1}$ and 67.3 $kJmol^{-1}$ of the lowest energy conformer. The equilibrium geometry of **A** was refined using molecular mechanics energy minimization methods (MMFF94) within *Spartan '14* and used as the starting geometry for gas phase DFT calculations (B3LYP/6-311G*). The same method was applied to structure **E**. Analysis of 72 conformers again resulted in two groups being retained: a cluster of 14 very similar structures within 7.9 $kJmol^{-1}$ of the lowest energy conformer a second cluster of 15 structures related to structure **F** with energies between 63.0 $kJmol^{-1}$ and 71.3 $kJmol^{-1}$ of the lowest energy conformer. The same method was applied to structure **G**. Analysis of 72 conformers again resulted in two groups being retained: a cluster of 14 very similar structures within 8.0 $kJmol^{-1}$ of the lowest energy conformer a second cluster of 16 structures related to structure H with energies between 57.2 $kJmol^{-1}$ and 65.4 $kJmol^{-1}$ of the lowest energy conformer. Tautomers **C**, **D** and **H** were unstable and reverted to stuctures **A**, **B** and **G**, respectively. MMFF94-derived structures were used as inputs for DFT calculations as before. First excited (triplet) states were computed as above but using a time-dependent density functional (TDDFT) model as implemented in *Spartan '14*, also using B3LYP/6-311G* in a vacuum.

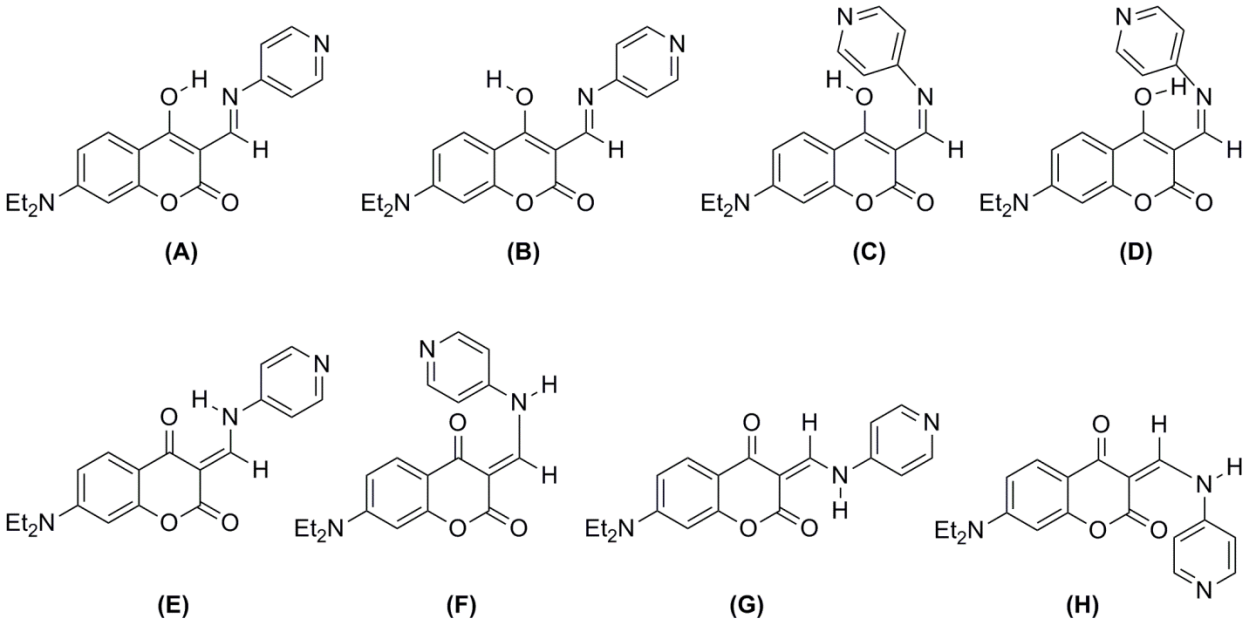

Figure S35: Possible tautomers for molecular probe **3**.

Cyanide addition

A sequence of structures was generated in which CN^- approached the target carbon down a vector. A reaction trajectory was attempted using DFT/B3LYP/6-311G*but simulations resulted in proton abstraction rather than cyanide addition so a simpler method was employed. A trial semiempirical simulation indicated that there were no orbital interactions between CN^- and the target at distances exceeding 3.147 Å for both reactions. This was taken as a starting point and the C-CN distance was reduced in steps of 0.333 Å down to 1.480 Å which had been identified as the optimum C-CN bond distance from a DFT/B3LYP/6-311G*calculation. At each step the C-CN distance was constrained by freezing the positions of both carbon atoms and the C-CN angle was constrained to 180°. With these constraints, geometry optimisation was undertaken using molecular mechanics (MMFF94). To account for the transition between the initial system in which CN^- has no interaction with the neutral target to that in which CN is covalently linked and the negative charge has migrated to the phenol, three models were used. In the first both oxygens were given a formal double bond (I), in the last all bond migrations had occurred (III) and in the intermediate four structures delocalised bonds were set (II). The resulting structures were used to generate molecular orbitals at a semiempirical (PM6) level.

Table S6. Frontier molecular orbital energies for stable conformers.

		A	**B**	**E**	**F**	**G**
Ground state	HOMO	-5.811	-5.850	-5.672	-5.641	-5.745
	LUMO	-2.247	-2.150	-2.307	-2.147	-2.270
First excited state	α-HOMO	-3.266	-3.278	-3.342	-3.208	-3.140
	α-LUMO	-1.261	-1.061	-1.195	-1.039	-1.308
	β-HOMO	-6.167	-6.114	-5.860	-5.617	-5.617
	β-LUMO	-4.722	-4.641	-4.878	-5.061	-5.061
ΔE(eV)		0.000	-0.039	0.139	0.170	0.066
ΔE(kJmol^{-1})		0.000	-3.763	13.41	16.40	6.37

Table S7. Frontier molecular orbital energy changes during C-CN bond formation.

Orbital energy (eV)	C···CN$^-$ distance (Å)					
	3.147	2.813	2.480	2.147	1.813	1.480
X = N						
LUMO	1.72	1.73	2.06	2.41	2.62	2.65
HOMO	-2.98	-3.54	-4.27	-5.20	-5.59	-5.45
X = CH						
LUMO	1.93	1.97	2.27	2.53	2.66	2.90
HOMO	-2.81	-3.35	-4.07	-4.98	-5.17	-5.29

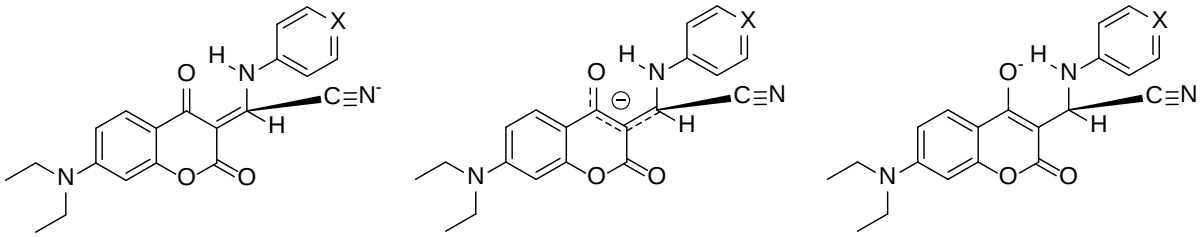

Figure S36. Representations of structures used to generate input geometries for MMFF94/PM6 calculations (X = N or CH).

X-Ray Tables

Crystal data for **3**, $C_{19}H_{19}N_3O_3$, *M* =337.37, yellow lath, 0.42 × 0.09 × 0.02 mm^3, triclinic, space group *P*-1 (No. 2), *a* = 5.0790(4), *b* = 12.8141(10), *c* = 13.2671(9) Å, α = 70.308(5), β = 80.767(5), γ = 88.005(5)°, *V* = 802.26(10) $Å^3$, *Z* = 2, D_c = 1.397 g/cm^3, F_{000} = 356, μ = 0.786 mm^{-1}, Bruker Kappa APEX-II DUO, CuKα radiation, λ = 1.54184 Å, *T* = 100.0(5)K, $2\theta_{max}$ = 127.8º, 9920 reflections collected, 2566 unique (R_{int} = 0.0388). Final *GOF* = 1.100, *R1* = 0.0454, *wR2* = 0.1301, *R* indices based on 2245 reflections with I>2σ(I) (refinement on F^2), 250 parameters, 2 restraints. Lp and absorption corrections applied, $\Delta\rho_{max}$ = 0.25 $eÅ^{-3}$, $\Delta\rho_{min}$ = -0.31 $eÅ^{-3}$.

supplementary materials

Computing details

Data collection: Bruker *APEX2*; cell refinement: Bruker *SAINT*; data reduction: Bruker *SAINT*; program(s) used to solve structure: *SHELXS97* (Sheldrick, 2008); program(s) used to refine structure: *SHELXL97* (Sheldrick, 2008); molecular graphics: *ORTEP-3 for Windows* (Farrugia, 2012); software used to prepare material for publication: *SHELXL97* (Sheldrick, 2008).

(Compound 3)

Crystal data

$C_{19}H_{19}N_3O_3$
$M_r = 337.37$
Triclinic, $P\overline{1}$
Hall symbol: -P 1
$a = 5.0790$ (4) Å
$b = 12.8141$ (10) Å
$c = 13.2671$ (9) Å
$\alpha = 70.308$ (5)°
$\beta = 80.767$ (5)°
$\gamma = 88.005$ (5)°
$V = 802.26$ (10) Å^3
$Z = 2$
$F(000) = 356$
$D_x = 1.397$ Mg m^{-3}
Cu $K\alpha$ radiation, $\lambda = 1.54184$ Å
Cell parameters from 3404 reflections
$\theta = 3.6$–$63.6°$
$\mu = 0.79$ mm^{-1}
$T = 100$ K
Lath, yellow
0.42 × 0.09 × 0.02 mm

Data collection

Bruker Kappa APEX-II DUO diffractometer
Radiation source: IμS microfocus
QUAZAR multilayer optics monochromator
φ and ω scans
Absorption correction: multi-scan TWINABS (Sheldrick, 2004)
$T_{min} = 0.734$, $T_{max} = 0.985$
9920 measured reflections
2566 independent reflections
2245 reflections with $I > 2\sigma(I)$
$R_{int} = 0.039$
$\theta_{max} = 63.9°$, $\theta_{min} = 3.6°$
$h = -5 \rightarrow 5$
$k = -13 \rightarrow 14$
$l = 0 \rightarrow 15$

Refinement

Refinement on F^2
Least-squares matrix: full
$R[F^2 > 2\sigma(F^2)] = 0.045$
$wR(F^2) = 0.141$
$S = 1.10$
2566 reflections
250 parameters
2 restraints
Primary atom site location: structure-invariant direct methods
Secondary atom site location: difference Fourier map
Hydrogen site location: inferred from neighbouring sites
H atoms treated by a mixture of independent and constrained refinement
$w = 1/[\sigma^2(F_o^2) + (0.0953P)^2 + 0.1126P]$ where $P = (F_o^2 + 2F_c^2)/3$
$(\Delta/\sigma)_{max} < 0.001$
$\Delta\rho_{max} = 0.25$ e Å^{-3}
$\Delta\rho_{min} = -0.31$ e Å^{-3}

Special details

Refinement
Refinement of F^2 against ALL reflections. The crystal was a nonmerohedral twin by 180 °. rotation about the reciprocal 0 0 1 axis. Refinement was against HKLF 5 data, and the BASF parameter refined to 0.425 (2).

Fractional atomic coordinates and isotropic or equivalent isotropic displacement parameters (Å²)

	x	*y*	*z*	U_{iso}*/U_{eq}	Occ. (<1)
O1	0.5386 (3)	0.61811 (11)	0.59765 (10)	0.0170 (4)	
O2	0.2451 (3)	0.56753 (12)	0.51698 (11)	0.0202 (4)	
O3	0.3942 (3)	0.33335 (12)	0.86339 (11)	0.0202 (4)	
N1	0.0529 (4)	0.27177 (15)	0.76225 (15)	0.0185 (4)	
H1N	0.134 (5)	0.258 (2)	0.817 (2)	0.022*	
N2	−0.5013 (4)	0.02793 (15)	0.77850 (16)	0.0265 (5)	
N3	1.1587 (5)	0.75856 (16)	0.75483 (15)	0.0312 (5)	
C1	0.3523 (4)	0.54285 (17)	0.59646 (16)	0.0168 (5)	
C2	0.3029 (4)	0.44117 (17)	0.68960 (16)	0.0158 (5)	
C3	0.4358 (4)	0.42014 (17)	0.78321 (16)	0.0157 (5)	
C4	0.6218 (4)	0.50614 (17)	0.77762 (16)	0.0151 (5)	
C5	0.6688 (4)	0.60091 (17)	0.68585 (16)	0.0159 (5)	
C6	0.8441 (4)	0.68418 (17)	0.67643 (16)	0.0182 (5)	
H6	0.8707	0.7470	0.6121	0.022*	
C7	0.9843 (5)	0.67681 (17)	0.76172 (16)	0.0192 (5)	
C8	0.9382 (4)	0.58062 (17)	0.85588 (16)	0.0185 (5)	
H8	1.0300	0.5729	0.9149	0.022*	
C9	0.7633 (4)	0.49910 (17)	0.86228 (16)	0.0175 (5)	
H9	0.7365	0.4356	0.9260	0.021*	
C10	0.1190 (4)	0.36805 (17)	0.68350 (16)	0.0169 (5)	
H10	0.0358	0.3870	0.6206	0.020*	
C11	−0.1308 (4)	0.19165 (17)	0.76406 (17)	0.0179 (5)	
C12	−0.2766 (5)	0.20437 (18)	0.68084 (18)	0.0214 (5)	
H12	−0.2537	0.2684	0.6176	0.026*	
C13	−0.4566 (5)	0.12070 (18)	0.69297 (18)	0.0253 (5)	
H13	−0.5563	0.1301	0.6358	0.030*	
C14	−0.3548 (5)	0.01738 (18)	0.85654 (18)	0.0237 (5)	
H14	−0.3799	−0.0481	0.9183	0.028*	
C15	−0.1694 (5)	0.09530 (18)	0.85344 (18)	0.0201 (5)	
H15	−0.0705	0.0831	0.9113	0.024*	
C16	1.2553 (11)	0.8462 (4)	0.6506 (4)	0.0199 (14)	0.546 (8)
H16A	1.2515	0.8190	0.5893	0.024*	0.546 (8)
H16B	1.4405	0.8693	0.6488	0.024*	0.546 (8)
C17	1.0688 (10)	0.9425 (5)	0.6433 (4)	0.0237 (13)	0.546 (8)
H17A	1.1265	1.0035	0.5757	0.036*	0.546 (8)
H17B	1.0724	0.9676	0.7051	0.036*	0.546 (8)
H17C	0.8869	0.9187	0.6442	0.036*	0.546 (8)
C16A	1.1112 (13)	0.8769 (6)	0.6809 (4)	0.0181 (15)	0.454 (8)
H16C	0.9255	0.8840	0.6659	0.022*	0.454 (8)
H16D	1.1438	0.9316	0.7156	0.022*	0.454 (8)
C17A	1.3075 (11)	0.8956 (5)	0.5768 (5)	0.0296 (18)	0.454 (8)
H17D	1.2867	0.9704	0.5264	0.044*	0.454 (8)
H17E	1.2724	0.8408	0.5436	0.044*	0.454 (8)
H17F	1.4900	0.8876	0.5932	0.044*	0.454 (8)
C18	1.3080 (5)	0.75110 (18)	0.84227 (16)	0.0199 (5)	
H18A	1.4702	0.7990	0.8117	0.024*	
H18B	1.3661	0.6738	0.8729	0.024*	
C19	1.1499 (5)	0.78513 (18)	0.93317 (18)	0.0221 (5)	
H19A	1.1125	0.8644	0.9058	0.033*	
H19B	1.2539	0.7704	0.9925	0.033*	
H19C	0.9815	0.7425	0.9598	0.033*	

Atomic displacement parameters (Å²)

	U^{11}	U^{22}	U^{33}	U^{12}	U^{13}	U^{23}
O1	0.0205 (9)	0.0150 (7)	0.0160 (7)	−0.0034 (6)	−0.0045 (6)	−0.0047 (6)
O2	0.0242 (9)	0.0210 (8)	0.0169 (7)	−0.0009 (7)	−0.0079 (6)	−0.0062 (6)
O3	0.0230 (9)	0.0165 (8)	0.0190 (8)	−0.0042 (6)	−0.0027 (6)	−0.0030 (6)
N1	0.0196 (11)	0.0179 (10)	0.0198 (9)	−0.0002 (8)	−0.0051 (8)	−0.0077 (8)
N2	0.0245 (12)	0.0201 (10)	0.0354 (11)	−0.0041 (9)	−0.0046 (9)	−0.0095 (8)
N3	0.0477 (14)	0.0213 (11)	0.0222 (10)	−0.0198 (10)	−0.0154 (9)	0.0024 (8)
C1	0.0167 (12)	0.0166 (10)	0.0194 (10)	0.0001 (9)	0.0003 (9)	−0.0105 (9)
C2	0.0146 (12)	0.0157 (10)	0.0181 (10)	0.0009 (9)	−0.0009 (9)	−0.0080 (8)
C3	0.0143 (12)	0.0142 (10)	0.0177 (10)	0.0008 (9)	0.0008 (8)	−0.0058 (9)
C4	0.0117 (11)	0.0168 (11)	0.0193 (10)	0.0015 (9)	−0.0028 (8)	−0.0092 (8)
C5	0.0163 (12)	0.0170 (11)	0.0159 (10)	0.0027 (9)	−0.0032 (8)	−0.0074 (9)
C6	0.0235 (13)	0.0140 (10)	0.0154 (10)	−0.0033 (9)	−0.0024 (9)	−0.0028 (8)
C7	0.0212 (13)	0.0174 (11)	0.0205 (11)	−0.0014 (10)	−0.0034 (9)	−0.0081 (9)
C8	0.0208 (13)	0.0196 (11)	0.0161 (10)	0.0013 (9)	−0.0054 (9)	−0.0061 (9)
C9	0.0192 (12)	0.0140 (10)	0.0172 (10)	−0.0005 (9)	−0.0011 (8)	−0.0032 (8)
C10	0.0162 (12)	0.0171 (11)	0.0191 (10)	0.0023 (9)	−0.0012 (8)	−0.0092 (9)
C11	0.0143 (12)	0.0173 (11)	0.0244 (11)	0.0007 (9)	−0.0002 (9)	−0.0111 (9)
C12	0.0221 (13)	0.0164 (11)	0.0259 (11)	0.0002 (10)	−0.0056 (9)	−0.0063 (9)
C13	0.0261 (14)	0.0210 (12)	0.0296 (13)	−0.0004 (10)	−0.0077 (10)	−0.0079 (10)
C14	0.0242 (14)	0.0156 (11)	0.0281 (12)	−0.0024 (10)	−0.0006 (10)	−0.0045 (9)
C15	0.0185 (13)	0.0199 (11)	0.0229 (11)	0.0005 (10)	−0.0031 (9)	−0.0087 (9)
C16	0.016 (3)	0.023 (3)	0.021 (3)	−0.003 (2)	−0.002 (2)	−0.009 (3)
C17	0.027 (3)	0.020 (3)	0.023 (2)	0.001 (2)	−0.0082 (19)	−0.004 (2)
C16A	0.021 (3)	0.012 (4)	0.020 (3)	0.000 (3)	−0.007 (3)	−0.002 (3)
C17A	0.031 (4)	0.030 (3)	0.018 (4)	−0.006 (3)	0.002 (2)	0.001 (3)
C18	0.0197 (13)	0.0194 (11)	0.0213 (11)	−0.0046 (9)	−0.0039 (9)	−0.0069 (9)
C19	0.0232 (14)	0.0180 (11)	0.0243 (11)	−0.0011 (10)	−0.0018 (9)	−0.0067 (9)

Geometric parameters (Å, º)

O1—C1	1.380 (3)	C11—C15	1.387 (3)
O1—C5	1.386 (2)	C11—C12	1.388 (3)
O2—C1	1.207 (3)	C12—C13	1.384 (3)
O3—C3	1.249 (2)	C12—H12	0.9500
N1—C10	1.332 (3)	C13—H13	0.9500
N1—C11	1.403 (3)	C14—C15	1.382 (3)
N1—H1N	0.86 (3)	C14—H14	0.9500
N2—C13	1.334 (3)	C15—H15	0.9500
N2—C14	1.338 (3)	C16—C17	1.515 (7)
N3—C7	1.365 (3)	C16—H16A	0.9900
N3—C18	1.460 (3)	C16—H16B	0.9900
N3—C16	1.479 (5)	C17—H17A	0.9800
N3—C16A	1.538 (7)	C17—H17B	0.9800
C1—C2	1.458 (3)	C17—H17C	0.9800
C2—C10	1.376 (3)	C16A—C17A	1.521 (7)
C2—C3	1.450 (3)	C16A—H16C	0.9900
C3—C4	1.452 (3)	C16A—H16D	0.9900
C4—C5	1.394 (3)	C17A—H17D	0.9800
C4—C9	1.404 (3)	C17A—H17E	0.9800
C5—C6	1.374 (3)	C17A—H17F	0.9800
C6—C7	1.407 (3)	C18—C19	1.519 (3)

C6—H6	0.9500	C18—H18A	0.9900
C7—C8	1.422 (3)	C18—H18B	0.9900
C8—C9	1.367 (3)	C19—H19A	0.9800
C8—H8	0.9500	C19—H19B	0.9800
C9—H9	0.9500	C19—H19C	0.9800
C10—H10	0.9500		

C1—O1—C5	121.71 (16)	N2—C13—C12	125.2 (2)
C10—N1—C11	127.1 (2)	N2—C13—H13	117.4
C10—N1—H1N	115.2 (17)	C12—C13—H13	117.4
C11—N1—H1N	117.6 (17)	N2—C14—C15	124.5 (2)
C13—N2—C14	115.5 (2)	N2—C14—H14	117.8
C7—N3—C18	122.00 (18)	C15—C14—H14	117.8
C7—N3—C16	121.8 (2)	C14—C15—C11	118.6 (2)
C18—N3—C16	114.7 (2)	C14—C15—H15	120.7
C7—N3—C16A	117.6 (3)	C11—C15—H15	120.7
C18—N3—C16A	115.4 (2)	N3—C16—C17	106.4 (4)
O2—C1—O1	116.27 (18)	N3—C16—H16A	110.5
O2—C1—C2	125.7 (2)	C17—C16—H16A	110.5
O1—C1—C2	117.99 (18)	N3—C16—H16B	110.5
C10—C2—C3	122.49 (19)	C17—C16—H16B	110.5
C10—C2—C1	115.67 (19)	H16A—C16—H16B	108.6
C3—C2—C1	121.83 (19)	C16—C17—H17A	109.5
O3—C3—C2	122.2 (2)	C16—C17—H17B	109.5
O3—C3—C4	122.06 (19)	H17A—C17—H17B	109.5
C2—C3—C4	115.73 (18)	C16—C17—H17C	109.5
C5—C4—C9	116.6 (2)	H17A—C17—H17C	109.5
C5—C4—C3	120.69 (19)	H17B—C17—H17C	109.5
C9—C4—C3	122.71 (19)	C17A—C16A—N3	105.9 (5)
C6—C5—O1	115.15 (18)	C17A—C16A—H16C	110.6
C6—C5—C4	122.86 (19)	N3—C16A—H16C	110.6
O1—C5—C4	122.0 (2)	C17A—C16A—H16D	110.6
C5—C6—C7	120.25 (19)	N3—C16A—H16D	110.6
C5—C6—H6	119.9	H16C—C16A—H16D	108.7
C7—C6—H6	119.9	C16A—C17A—H17D	109.5
N3—C7—C6	121.53 (19)	C16A—C17A—H17E	109.5
N3—C7—C8	120.97 (19)	H17D—C17A—H17E	109.5
C6—C7—C8	117.5 (2)	C16A—C17A—H17F	109.5
C9—C8—C7	120.7 (2)	H17D—C17A—H17F	109.5
C9—C8—H8	119.7	H17E—C17A—H17F	109.5
C7—C8—H8	119.7	N3—C18—C19	113.7 (2)
C8—C9—C4	122.1 (2)	N3—C18—H18A	108.8
C8—C9—H9	118.9	C19—C18—H18A	108.8
C4—C9—H9	118.9	N3—C18—H18B	108.8
N1—C10—C2	122.6 (2)	C19—C18—H18B	108.8
N1—C10—H10	118.7	H18A—C18—H18B	107.7
C2—C10—H10	118.7	C18—C19—H19A	109.5
C15—C11—C12	118.4 (2)	C18—C19—H19B	109.5
C15—C11—N1	118.5 (2)	H19A—C19—H19B	109.5
C12—C11—N1	123.1 (2)	C18—C19—H19C	109.5
C13—C12—C11	117.9 (2)	H19A—C19—H19C	109.5
C13—C12—H12	121.1	H19B—C19—H19C	109.5
C11—C12—H12	121.1		

Hydrogen-bond geometry (Å, º)

D—H···*A*	*D*—H	H···*A*	*D*···*A*	*D*—H···*A*
N1—H1*N*···O3	0.86 (3)	1.95 (3)	2.642 (2)	137 (2)
C10—H10···O2^{i}	0.95	2.40	3.342 (3)	170
C12—H12···O2^{i}	0.95	2.25	3.191 (3)	171

Symmetry code: (i) −*x*, −*y*+1, −*z*+1.

References:

1. M. Cigáň; J. Donovalová; V. Szöcs; J. Gašpar; K. Jakusová; A. Gáplovský, *J. Phys. Chem. A* 2013, *117*, 4870.
2. Wavefunction, Inc.: Irvine, CA, 2014.